cosmetics

MDPI

Article

Bleached Hair as Standard Template to Insight the Performance of Commercial Hair Repair Products

Eva Martins [1,*], Pedro Castro [1], Alessandra B. Ribeiro [1], Carla F. Pereira [1], Francisca Casanova [1], Rui Vilarinho [2], Joaquim Moreira [2] and Óscar L. Ramos [1]

[1] CBQF-Centro de Biotecnologia e Química Fina-Laboratório Associado, Escola Superior de Biotecnologia, Universidade Católica Portuguesa, Rua Diogo Botelho 1327, 4169-005 Porto, Portugal; oramos@ucp.pt (Ó.L.R.)
[2] Institute of Physics for Advanced Materials, Nanotechnology and Photonics (IFIMUP), Physics and Astronomy Department, Faculty of Sciences, University of Porto, Rua do Campo Alegre s/n, 4169-007 Porto, Portugal
* Correspondence: eva.biotec@gmail.com or elgraca@ucp.pt

Abstract: The increasing demand for effective hair care products has highlighted the necessity for rigorous claims substantiation methods, particularly for products that target specific hair types. This is essential because the effectiveness of a product can vary significantly based on the hair's condition and characteristics. A well-defined bleaching protocol is crucial for creating a standardized method to assess product efficacy, especially for products designed to repair damaged hair. The objective of this study was to create a practical bleaching protocol that mimics real-world consumer experiences, ensuring that hair samples exhibit sufficient damage for testing. This approach allows for a reliable assessment of how well various products can repair hair. The protocol serves as a framework for evaluating hair properties and the specific effects of each product on hair structure. Color, brightness, lightness, morphology, and topography were primarily used to understand the big differences in the hair fiber when treated with two repair benchmark products, K18® and Olaplex®, in relation to the Bleached hair. The devised bleaching protocol proved to be a fitting framework for assessing the properties of hair and the unique characteristics of each tested product within the hair fiber. This protocol offers valuable insights and tools for substantiating consumer claims, with morphological and mechanical methods serving as indispensable tools for recognizing and validating claims related to hair. The addition of K18® and Olaplex® demonstrated an increase in hair brightness (Y) and lightness (L* and a*) in relation to the Bleached samples, which were considered relevant characteristics for consumers. Olaplex®'s water-based nature creates a visible inner sheet, effectively filling empty spaces and improving the disulfide linkage network. This enhancement was corroborated by the increased number of disulfide bonds and evident changes in the FTIR profile. In contrast, K18®, owing to the lipophilic nature of its constituents, resulted in the formation of an external layer above the fiber. The composition of each of the products had a discrete impact on the fiber distribution, which was an outcome relevant to the determination of spreadability by consumers.

Keywords: hair fibers; bleaching; hair repair; fiber length characterization; potential claims

Citation: Martins, E.; Castro, P.; Ribeiro, A.B.; Pereira, C.F.; Casanova, F.; Vilarinho, R.; Moreira, J.; Ramos, Ó.L. Bleached Hair as Standard Template to Insight the Performance of Commercial Hair Repair Products. *Cosmetics* **2024**, *11*, 150. https://doi.org/10.3390/cosmetics11050150

Academic Editor: Vasil Georgiev

Received: 24 July 2024
Revised: 19 August 2024
Accepted: 22 August 2024
Published: 28 August 2024

1. Introduction

Healthy and attractive hair is often linked to overall well-being, which drives individuals to invest in hair care products. This trend is projected to expand the market from $99.53 billion in 2023 to $147.49 billion by 2030, with a CAGR of 5.8% during the forecast period [1]. Advances in cosmetic science have led to the development of innovative formulations, including ingredients like keratin, argan oil, biotin, vitamins, and minerals that claim to promote healthier hair [2]. Hair care products can interact differently on the hair surface at the micro- and macroscopic levels depending on several factors, such as human

race, hair type, age, and environmental conditions. External elements like pollution or chemical treatments further contribute to this complexity. These interactions play a role in surface roughness, friction, and adhesion, ultimately impacting the consumer's perception of the product's effectiveness and suitability for their specific needs [2–5]. Moreover, certain diseases and malnutrition may negatively impact hair health, from the genesis of the hair follicle to the erosion of physiological chemical structures [6,7]. Therefore, it is critical for the cosmetic industry to understand the attributes that mostly influence consumers' perceptions of the quality and efficacy of hair care products [8–10]. Bleaching is a frequent hair treatment widely used in the cosmetic industry and in hairdressers' salons with a relevant influence on hair properties, denoting the alterations of lightening the hair by a shade or two beyond its original color, leading to noticeable alterations in its appearance [1]. It works by stripping the hair of its natural pigment (melanin) using alkaline treatment and an oxidizing agent.

Alkaline treatment (e.g., ammonium hydroxide) is usually the first step in the bleaching process, after which an oxidizing chemical (e.g., hydrogen peroxide) is applied [11]. This combination raises the pH of the hair and disrupts the cuticle (the outermost layer of the hair shaft), making it more porous and leading to further mechanical damage. This allows hydrogen peroxide to penetrate and reach the cortex, where melanin resides. Once inside, hydrogen peroxide oxidizes melanin in the hair, breaking it down and removing color. The longer the bleach is left on, the more melanin is broken down, leading to lighter hair. The extent of lightening depends on the concentration of hydrogen peroxide, the time it is left on the hair, and the natural hair color [12]. Therefore, the bleaching process involves dissolving the melanin pigment, which is responsible for hair color [13,14]. Melanin granules begin to break down and leak into the intermacrofibrillar matrix as a result of bleaching [15]. Because of the catalytic action of hydrogen peroxide in the bleaching agents outside the melanin granules, the diffusion of metal elements into the intermacrofibrillar matrix encouraged deeper damage to the hair [15]. As a result, bleaching can cause the break down the protein structure (keratin) in the cortex, and hair can lose flexibility and become dry, brittle and harsh [16,17]. Hydrogen peroxide not only breaks down melanin but can also affect the disulfide bonds within the keratin structure, leading to weakened and brittle hair.

In addition, hair bleaching and coloring have been proven to drastically accelerate cuticle degeneration across the full fiber length [4]. Bleaching and other oxidative treatments cause cuticle cells to break down and cause deterioration of the strong disulfide linkages in hair fibers [18,19]. The oxidizing agents present in the hair dye and bleach disrupt the keratin disulfide bonds, forming cysteic acid, resulting in a reduction in keratin structural rigidity and the extent of disulfide bond breakage. However, pre-treating hair with bleaching agents improves dye absorption and increases hair fiber accessibility for later treatments [15,20]. It is crucial to investigate cosmetic ingredients for hair repair and to enhance the physical characteristics of hair, particularly its mechanical qualities [17].

Bleaching can significantly alter and damage hair [21]; however, there are effective methods to repair and maintain hair health. Protein treatments, deep conditioning, pH balancing, and bond-building products are practical ways to preserve the integrity of bleached hair [12,22].

Protein treatments help restore hair strength by temporarily filling in gaps in the cuticle caused by the loss of keratin [23,24]. These treatments typically contain hydrolyzed proteins, which are small enough to penetrate the cuticle and reinforce the hair structure [25]. The use of innovative ingredients such as keratin peptides [25], proteins such as silk and collagen [21], and amino acids [26], and the development of active formulations to repair hair damage have received a lot of attention, mostly through the repair of chemical bonds [27]. Deep conditioning treatments focus on replenishing the moisture lost during the bleaching process. These treatments usually contain emollients, humectants, and oils that help to hydrate and smooth the hair cuticle, reduce porosity, and increase shine. Ingredients, such as shea butter, coconut oil, and glycerin, are commonly found in these

products [28]. After bleaching, the hair cuticle may remain raised, leading to increased porosity and moisture loss [29]. Acidic products or pH-balanced conditioners help to lower the hair's pH and reseal the cuticle. This reduces frizz and helps retain moisture [30–32]. Maintaining the hair's natural pH (around 4.5 to 5.5) is crucial for minimizing damage and maintaining shine [30,33]. Bond builders function by identifying and restoring disulfide bonds that are damaged as a result of chemical reactions such as bleaching. These products contain active ingredients which reconnect the broken bonds, helping to restore the hair's strength and elasticity and improve the overall health of bleached hair [22,34]

Hair health and appearance are the result of a complex plethora of interrelatable physicochemical and biological characteristics [35,36]. Human hair is composed of a well-organized group of fibers mainly constituted of proteins (>90%), in particular keratin, but also lipids (1–9%) and minerals (of which calcium, magnesium, sodium, and potassium are usually the main ones <1%) [5]. Proteins and lipids can be classified as exogenous or endogenous based on whether they originate from hair matrix cells or sebaceous glands, respectively [37]. Moreover, human hair's basic structure comprises a central medulla region that is surrounded by a cortex, which is covered by a lipid cuticle layer and contains the majority of the hair's keratin (a structural protein) and melanin [38,39]. In the external region of hair strands, the cuticle acts as the first protective barrier against exogenous materials due to the presence of an outer hydrophobic epicuticle consisting of a monolayer of 18-methyl eicosanoic fatty acids [40,41]. The epicuticle also contains flattened cells over the polyhedral cortical cells that gather with the lipid layer and are responsible for the brightness, glossiness, and texture of the hair [42,43]. Several studies have demonstrated that the outermost cuticle cells play a role in the appearance of human hair as the first surface line in contact with physical and chemical external aggression [8,44,45]. The condition of the cuticle layer assumes morphological and mechanical characteristics that can help diagnose diseases and monitor certain hair treatments [46]. Once the hair surface is damaged, repair is typically limited by external measures. Beneath the epicuticle, the cortex is mainly composed of keratin filaments embedded within spindle-like cortical cells. Additionally, a protein matrix with a high cysteine content (among which pairs of keratin polypeptide chains form rigid protofilaments) is blended in the cortex area. Hair rigidity is directly related to the fact that keratin filaments form disulfide bonds, thus establishing strong connections between adjacent keratin chains that are responsible for the tensile and textural characteristics of the hair [47,48]. Consequently, changes in the mechanical properties of hair may be related to the disruption of disulfide bonds. It is interesting to note that the main element of hair fibers that affects their mass, volume, and associated mechanical characteristics is the cortex [49,50]. The innermost hair layer (or the medulla) is composed of round cells in thicker hair, but may also be almost devoid of content or even absent (in the fine hair of children), fragmented, or continuous [28,51,52].

This study aims to present a bleaching protocol that revealed measurable and noticeable hair damage in Caucasian hair, establishing it as a suitable foundation for testing formulations related to hair beauty, as well as providing a thorough guideline for the analytical methodology to evaluate the impact of innovative beauty products such as K18® and Olaplex® on the repair properties of bleached damaged hair. Moreover, it provides insight into the intrinsic changes in the fiber structure, such as the S-S bonds, after a single application of repair products, relating them to hair fiber appearance, morphology, and thermal, structural, and mechanical properties. This research may offer perspectives on the topic of hair repair, validate the functional properties of commercial hair products, and support their claims and role in hair fiber.

2. Materials and Methods

2.1. Hair Type

The hair samples used in this study were bleached Caucasian hair purchased from Kerling International Haarfabrik GmbH (Stuttgart, Germany). The company sells certified hair tresses that meet the standardized quality, ensuring that they are suitable for evaluating

hair treatments. It was supplied as large tresses, 25 cm long and 4 g in weight, constructed with rectangular pieces of wax that secured the root ends of the hair fiber. The bleached treatment applied by the supplier comprised a washing step with 2% (*w*/*w*) hydrogen peroxide (H_2O_2) solution for 4 h at 38 °C, followed by the application of sodium persulfate ($Na_2S_2O_8$). Since no visible damage was observed in these samples by Scanning Electron Microscopy (SEM), as detailed below, an additional bleaching procedure was implemented to ensure that real damage was caused to the hair fiber surface. This condition is mandatory for evaluating the repair potential of commercial products.

2.2. Commercial Repair Products

K18®, used as a molecular repair hair mask, was purchased from Biomimetic HairScience (Los Angeles, CA, USA). It is composed of water, alcohol denat., propylene glycol, cetearyl alcohol, dicaprylyl ether, cetyl esters, behentrimonium chloride, polysorbate 20, sh-oligopeptide-78, hydrolyzed wheat protein, hydrolyzed wheat starch, isopropyl alcohol, tocopherol, phenoxyethanol, potassium sorbate, citric acid, fragrance (parfum), geraniol, linalool, hexyl cinnamal, and benzyl alcohol, according to the manufactured information.

Olaplex® N°0, used as an intensive bond-building agent, was purchased from OLAPLEX Bond Building Technology (Santa Barbara, CA, USA). This product is composed of water, bis-aminopropyl diglycol dimaleate, phenoxyethanol, and sodium benzoate, according to the manufacturer's information.

2.3. Hair Treatment

Bleaching protocol: To ensure noticeable damage to the hair fiber surface, a second bleaching procedure was carried out to mimic the salon bleach treatment. For this purpose, Bleach, Lights powder, and a developer (H_2O_2) at 40 vol., both obtained from LISAP MILANO Laboratori Cosmetici S.p.A. (Rescaldina, Italy), were mixed in a 1:1 ratio (*w*/*w*). Each hair stress was then vigorously massaged for 30 s with the premixed formulation, brushed five times, wrapped in aluminum foil, and left on for 50 min at 25 °C. The samples were washed for 30 s with tap water, and excess water was removed with absorbent paper.

Reset protocol: Before the application of the two commercial products under testing, all bleached hair samples were rinsed with a 10% (*w*/*v*) Sodium Lauryl Sulfate (SLS, Acofarma®) solution at a ratio of 20% in relation to tress hair weight (*w*/*w*), with a digital massage for 120 s. Following a 2 min leave-in period at room temperature, each tress was washed under tap water for 30 s, and the excess water was removed with a paper towel. The tresses were then brushed five times and oven-dried at 22 ± 2 °C and 55 ± 5% relative humidity (RH) for 24 h. This protocol served as a reset step to remove any exogenous impurities that may be present on the surface of the hair fibers, potentially affecting the results.

Leave-in K18® and Olaplex® application: 10% (*w*/*w*) of each product was applied to the optimized bleached hair samples with a digital massage for 1 min, left to react for 4 min, which was followed by 5 consecutive brushing steps to ensure a good distribution of each formulation on tresses (n = 3) and minimize any variability on application. After that, the tresses were stabilized in an oven at 22 ± 2 °C + 55 ± 5% RH for 48 h before testing.

2.4. Hair Characterization

Bleached, K18® and Olaplex® conditions were tested using bleached hair (standard damaged hair fiber), and in the case of K18® and Olaplex®, the bleached hair was treated with respective commercial formulations. A total of nine hair tresses were used for the experimental study, corresponding to three distinct hair tresses (n = 3) per condition. The middle section of each hair tress, with approximately 15 cm (excluding 5 cm from the top and 5 cm from the root), was used as a specimen for further analyses.

The commercial bleached samples were screened for the root, middle, and end regions of the hair fiber by Scanning Electron Microscopy (SEM) to understand if the bleached protocol applied by the supplier provoked visible damage to the fiber surface. As mentioned

earlier, no visible damage was observed by SEM; thus, an additional bleaching procedure was applied, and the sample was re-evaluated by SEM. This final sample presented appropriate damage and was used as a negative control and as an initial matrix to test the treatments with K18® and Olaplex®.

After the application of K18® and Olaplex® commercial products, the 3 conditions of hair tresses were characterized through the following techniques: hair appearance by photography; color, brightness, and lightness by colorimeter; surface morphology by SEM and by Atomic Force Microscopy (AFM); relative density by the gravimetric method using an analytical balance equipped with a density measurement apparatus; protein by quantitative determination of nitrogen using Dumas method; protein integrity and bonds by attenuated total reflection (ATR)- Fourier-transform infrared spectroscopy (FTIR), disulfide bonds by UV-Vis spectrophotometry, thermal properties by Differential Scanning Calorimetry (DSC) and Thermogravimetric Analysis (TGA), and mechanical properties by texture analyzer equipment.

2.4.1. Hair Appearance

Hair tress images were acquired using a 12-megapixel camera (iPhone Xs, Apple, Cupertino, CA, USA) with autofocus.

The Commission Internationale de l'Eclairage (CIE) defined CIELAB color as a standard tool for the determination of color changes in hair [53]. The CIELAB lightness (L*, a*, and b*) and brightness (Y) were performed using the CR-410 Chroma meter (from Minolta Chroma, Osaka, Japan) equipment.

The color parameters were used to determine the color point, in which L* corresponds to the luminosity coordinate (L* value is 100 for a white object and 0 for a black object); a* sets the green-red coordinate, and b* sets the blue-yellow color coordinate [54]. The color was measured on the surface of the hair stress had as background a white standard plate (L* = 93.22, a* = −0.08, and b* = 4.04), which was also used for the calibration of the equipment. The measurements were performed in three different hair tresses (middle region), with two technical replicates for each color parameter. The final values are presented as the mean ± SD of six individual measurements.

To diagnose the modifications between Bleached and other conditions, a normalization of the data was calculated according to Equation (1).

$$Normalization\ (\%) = \frac{Mt - Mb}{Mt} \times 100 \quad (1)$$

where, Mb is the mean of the bleached sample and Mt is the mean of the hair-treated sample.

2.4.2. Morphological Analysis

The surface morphology of hair samples was studied using SEM (Scanning Electron Microscope) and AFM (Atomic Force Microscopy). These techniques have complementary capabilities and allow the examination of the microstructure and morphology of hair fibers. SEM was performed using a Thermo Scientific™ Pro Scanning Electron Microscope (Waltham, MA, USA). For SEM observation, hair monofilaments (root, middle, and end regions) were mounted on stubs using double-sided carbon adhesive tape (NEM tape, Nisshin, Japan) and coated with Au/Pd (target SC510-314B from ANAME, S.L., Madrid, Spain) using a Sputter Coater (Polaron, Bad Schwalbach, Germany). All observations were performed in the high vacuum mode with an acceleration voltage of 5 or 10 kV. The fibers were surveyed at 1000×, 2500×, and 5000× magnifications, and all images presented were selected as representative of the hair morphology.

AFM was performed in the middle region of the hair fiber using BioAFM JPK NanoWizard 3 (Bruker, Billerica, MA, USA) equipment. For topography imaging, two measurements of each sample were performed in a 20 × 20 µm area. Beyond the evaluation of topography, AFM was used to measure the hair fiber surface properties such as Average Roughness—Ra

(nm), RMS Roughness—Rq (nm); and Peak to valley Roughness Rt (nm). The analyses were performed in the AC mode, and ACTA probes from AppNano were used. Plane leveling subtracting a polynomial (degree 1) surface from the image before roughness determination was performed.

2.4.3. Physical and Chemical Analysis

The relative density of the hair monofilament was determined using the method described in ASTM 792-20 with some modifications [55]. Each hair monofilament was weighed on a suspension apparatus plate, followed by the same hair monofilament on the apparatus plate immersed in pure water. The mass of the hair monofilament in air and water was used to calculate the relative density according to Equation (2):

$$p = \frac{m.px}{m - m1} \quad (2)$$

where r (g/cm^3) is the relative density of the hair monofilament, m (g) is the mass of the hair monofilament in air, $m1$ (g) is the mass of hair monofilament in water, and rx (g/cm^3) is the relative density of pure water at room temperature.

The amount of nitrogen (N_2) present in the hair was determined based on the Dumas method (AOAC Official Method 968.06) using Dumatec™ 8000/FOSS equipment (Hillerød, Denmark.). Briefly, the hair sample was cut into pieces ($\leq$0.5 mm), and around 100 mg was weighted into the aluminum foil crucible. Afterward, the sample was subjected to complete combustion at high temperatures in an oxygen atmosphere, generating molecular nitrogen. The calibration curve of ethylenediaminetetraacetic acid (EDTA; 10.9–150.2 mg) was used to calculate the concentration of nitrogen in the sample. The elemental content (N) was converted to protein concentration using the universal conversion factor (6.25), and the nitrogen content (%) was determined.

ATR-FTIR spectra of hair tresses were obtained using a Perkin Elmer infrared spectrometer (Frontier™ MIR/FIR spectrometer, Waltham, MA, USA) using an attenuated total reflection (ATR) accessory to provide a non-destructive measurement method. The samples were placed in direct contact with the ATR diamond by clamping the sample to ensure good optical contact. Subsequently, samples were scanned within the wave range of 550–4000 cm^{-1} for 128 scans/sample, a spectral resolution of 1 cm$^{-1,}$ and a scan speed of 0.2 scans/min.

Disulfide bond quantification was performed using Ellman's assay procedure [56]. Ellman's assay consists of the determination of free thiol groups before and after chemical reduction, and by subtracting the former from the latter. Briefly, 10 mg of hair samples were weighed and homogenized in 5 mL of 0.5 M phosphate buffer (pH 8.0). Next, 100 µL of Ellman's reagent solution (4 mg/mL) prepared in the same buffer was added to the mixture and further incubated at 37 °C in (water bath) for 24 h in the dark. The absorbance of the solution was measured using an EPOCH2 microplate reader (BioTek, Winooski, VT, USA) (λ = 412 nm). A L-cysteine calibration curve with concentrations ranging from 0.01 to 0.1 mg/mL was prepared (r^2 = 0.97), aiming to determine the accurate amount of free thiol groups in hair samples.

To determine the disulfide bond content, a complete reduction of disulfide bonds was performed using sodium borohydride ($NaBH_4$). In short, 10 mg of the hair sample was hydrated in 1.05 mL of deionized water for 10 min. After that, 450 µL of 0.05 M Tris buffer, pH 6.8, and 3.0 mL of freshly prepared 4% (w/v in 0.2 M NaOH) $NaBH_4$ solution were added to the hydrated hair sample solution. Then the solution was incubated in a shaking water bath at 37 $\pm$ 0.5 °C for 24 h. Afterward, the reduction reaction was inactivated by adding 600 µL of 5 M HCl under agitation for 10 min, and 6 mL of 1 M PBS (pH 8.0) was added to adjust the pH of the resulting reaction mixture. Finally, 200 µL of the sample and 20 µL of Ellman's reagent (4 mg/mL) were added to each well of a quartz 96-well plate. After shaking for 15 min at room temperature, the 96-well plate was quantified

by measuring the absorbance at 412 nm using a microplate reader. Nine replicates were performed for each experimental condition. The results are presented as mean ± SD.

For Raman spectroscopy analysis, spectra were recorded using an InVia™ Qontor® confocal Raman spectrometer (Wotton-under-Edge, UK) equipped with a Leica DM2700 microscope (Ernst Leitz GmbH, Wetzlar, Germany). A 50× objective was used to focus the laser beam on each measured diatom. The incident laser was a 532 nm Cobolt 04-01 Series Samba™ (Hübner Photonics, Kassel, Germany), regulated to 0.1 mW. Spectra were obtained with an acquisition time of 10 s and 3 accumulations. Raman spectra were acquired using WiRE™ 5.2 software (Renishaw Inc., Pontyclun, UK), and the area, width, and frequency variables fully describing a Raman band were estimated using a sum of damped oscillator functions in Igor Pro™ software (Version lgor Pro 4) (Wavemetrics Inc., Portland, OR, USA, 1998) without any signal processing.

2.4.4. Thermal Analysis

DSC analysis was performed under a nitrogen atmosphere using DSC 204 F1 Phoenix equipment from Netzsch (Selb, Germany), calibrated for temperature and enthalpy scale using an indium/zinc standard. The middle region of the hair fiber was cut into small portions and weighed (2–4 mg). Hair samples were then placed in aluminum DSC pans and sealed hermetically, with an empty pan used as a reference. The samples were then heated from 20 to 270 °C at a heating rate of 10 °C/min under an inert atmosphere by purging with nitrogen gas at a flow rate of 150 mL/min. The measurements were performed in three separate hair tresses, with two technical replicates for each.

TGA analysis was performed using STA7200 Simultaneous Thermal Analyzer equipment from Hitachi, (Tokyo, Japan). Approximately 3–3.2 mg of hair fiber (middle region) was placed in platinum pans and heated from 30 to 600 °C at 10 °C/min under a nitrogen atmosphere of 50 mL/min. The measurements were performed in two different hair tresses, with one technical replicate for each.

2.4.5. Mechanical Behavior

Individual hair tresses (ca. twenty-five monofilament hair fibers) were randomly selected from hair swatches to perform the mechanical tests using the TA. XT plus C Texture Analyzer. For this purpose, the thickness (μM) of the fibers was previously measured to comprehend the thickness variability and its impact on the mechanical properties of hair fibers. The thickness was determined by optical microscopy using an AxioImager.M2 fluorescence microscope (Zeiss, Oberkochen, Germany). Images were acquired, and the thickness of the directly mounted samples was determined using ZEISS ZEN 2012 software. Ruler calibration was performed using Primostar scales (Primovet scales at 5×, 10×, and 20× magnification).

Tensile strength and extensibility were calculated based on the average of all hair single fibers (normalization of results) using a load cell of 500 g and a clamping distance of 5.5 cm according to the ISO 5079:2020 [57]. Tension mode was selected, and the analysis was performed until hair breaking with a 5 mm/s test-speed, a 200 mm distance, and 20 g breaking sensitivity in the Exponent Connect (Version 8.0,16.0) Texture Analyzer software. All measurements were performed at room temperature (25 °C).

All the analytical tools for the characterization of hair are presented in Figure 1:

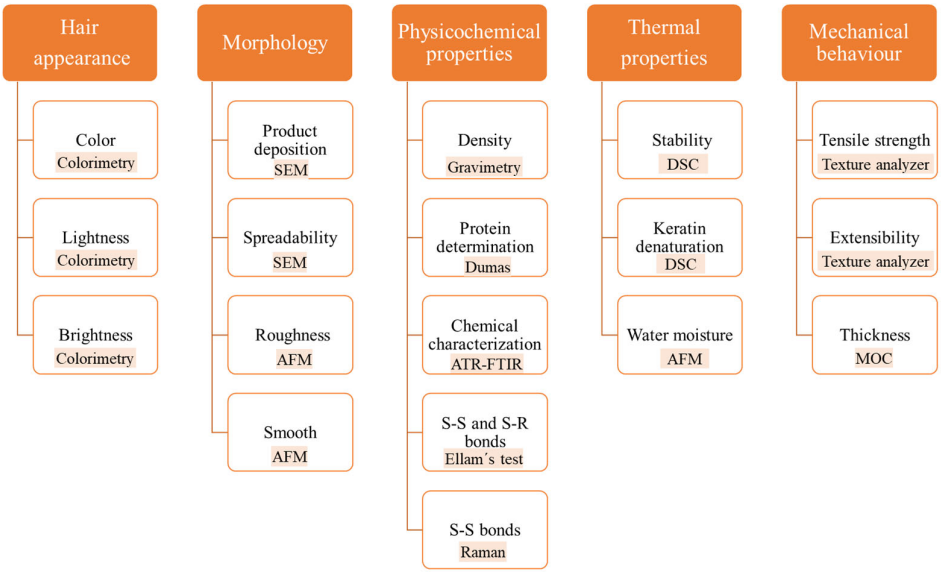

Figure 1. Analytical tools employed in this study for hair fiber characterization.

3. Statistical Analysis

Statistical analysis was performed by a two-way ANOVA followed by Tukey's post hoc test, using GraphPad Prism 8.0.1 (GraphPad Software, Inc., La Jolla, CA, USA). Differences between the Bleached, K18®, and Olaplex® hairs were assessed considering a confidence level of 95%. Statistical significance between the groups was verified by an asterisk (*) symbol at $p < 0.05$. All tests were conducted at least in triplicate ($n = 3$). The obtained data points are presented as mean ± standard deviation (Mean ± SD).

4. Results and Discussion

4.1. Hair Appearance

Regarding the visual appearance of hair fibers, the two commercial products showed macro color differences in relation to the control, which can be observed in Figure 2A. In the present work, the bleached hair showed a dry appearance without gloss compared to the K18® and Olaplex® samples. Moreover, tresses treated with both commercial products demonstrated good spreadability and combability behind their gloss appearance (Figure 2A). These key differentiators imply that hair post-application of the tested products revealed a pleasant experience, benefiting customer perception and satisfaction with the brands.

The parameters such as brightness (Y) and lightness using the system CIELAB (L*, a* b*) were measured in this study (Figure 2B–E). Hair color is an important criterion for hair beauty product consumers [58,59]. It has been previously reported that the L* (lightness), a* (red/green), and b* (yellow/blue) coordinates consistently increased after bleaching treatment [60].

From Figure 2B, it was observed that Olaplex® hair displayed the highest brightness value (40.60 ± 0.66) in relation to K18® (28.23 ± 0.90), both compared with bleached hair (26.60 ± 0.36). In fact, the Olaplex® and K18® products showed an increase in the brightness of ca. 34.5% and 5.8%, respectively, compared with bleached hair (Figure 2B(I)). Differences noted visually in brightness were confirmed by statistical analysis ($p < 0.05$). The same profile pattern was observed for the lightness (L*) (Figure 2C) and b* (Figure 2E) parameters. Olaplex® hair showed the highest L* (69.89 ± 0.47) and b* (28.45 ± 1.13) values compared to K18® (L* 60.09 ± 0.80; b* 27.75 ± 0.56) and bleached (L* 58.60 ± 0.34; b* 27.71 ± 1.23) hair samples. Olaplex® and K18® commercial products were able to significantly change ($p < 0.05$) the lightness by 16.2% and 2.5%, respectively, compared to bleached hair (Figure 2(C(II))). Considering the a* parameters that are related to the green-red coordinate, the opposite was observed, whereas the highest value was obtained for the bleached hair (9.02 ± 0.42), followed by K18® (8.39 ± 0.24) and Olaplex® (6.96 ± 0.17) hair (Figure 2D). Olaplex® and

K18® showed a decrease of 29.7% and 7.5%, respectively, in the a* color parameter compared with bleached hair (Figure 2(D(III))). In summary, Olaplex® hair was the formulation that most significantly boosted hair brightness and lightness compared to bleached hair. The presence of bis-aminopropyl diglycol dimaleate in Olaplex products has two vinyl endings that selectively react with free thiols to form an artificial, extended disulfide bridge. This has been reported to repair damaged hair and preserve its color [61,62]. This active ingredient demonstrated an effect on the hair's appearance, namely in color. It is interesting to note that the self-perception of customers in relation to hair color shows that component b* is the most important parameter describing variation, followed closely by L*. On the other hand, component a* seems to have very little influence on the consumer's color perception. Virgin hair is usually the matrix studied for the interpretation of the color parameter; it has been mentioned that there is a relationship between hair lightness and thickness [63]. Our results did not corroborate this statement, as the matrix reference for the color analysis was bleached hair.

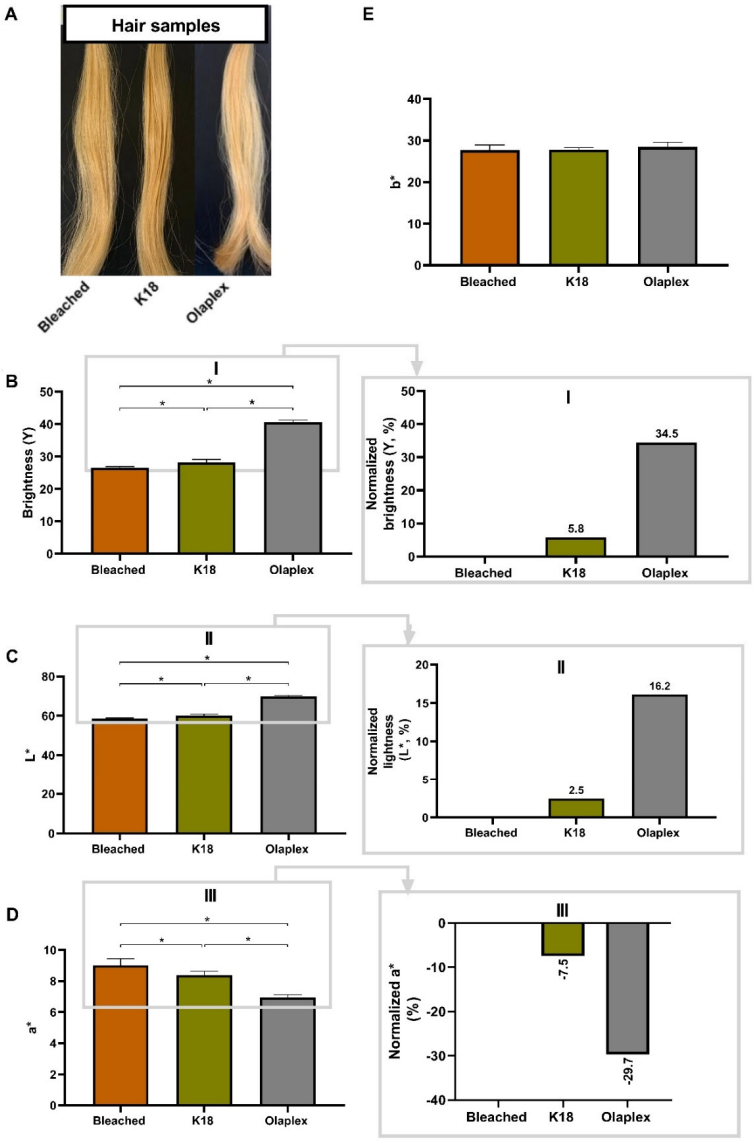

Figure 2. Photograph of hair tress appearance (**A**); hair tress brightness (Y) (**B**), lightness (**C**), a* (**D**), and b* (**E**) for K18® and Olaplex®-treated samples in comparison to bleached samples. The I, II, and III Roman numerals showed the variation of change for Y, L*, and a*, respectively, for hair tresses after the application of K18® or Olaplex® in relation to the bleached hair. Asterisks (*) denote a statistically significant difference ($p < 0.05$). Values represent the mean ± SD.

4.2. Morphological Analysis

To ascertain the extent of chemical damage induced by common bleaching agents and to evaluate the effectiveness of commercially available repair formulations, K18® and Olaplex®, a thorough physicochemical analysis was performed and reported in this study. This was undertaken to simulate conditions akin to those experienced by consumers and to assess the product's ability to improve the condition of hair subjected to diverse forms of damage. One of the most recurrent forms of hair damage is through the use of chemicals such as bleaching agents, which are reported to increase the permeability of hair [15,20]. Therefore, to evaluate the potential of the two commercial products widely recommended for hair repair, commercially bleached hair was used, which was divided into three sections: root, middle, and ends. In the very few published studies available on the effect of repair agents on damaged hair, the ends section is the region most studied, and it is by far the section with the clearest and most detectable hair damage. This can be attributed to it being the oldest hair fiber, which makes it more susceptible to and affected by external factors such as heat, pollution, UV, or brushing. Along with the gap in information about the remaining sections, it was decided to evaluate the full extension of the hair fiber morphology by SEM and AFM.

4.2.1. SEM Micrographic Analysis

Initially, the morphology of the hair sections was assessed using SEM micrographs (Figure 3A–I), allowing the examination of the entire hair fiber and the selection of an appropriate elite standard region for evaluating the repair effect. The purchased ends of the tresses used in this study give the impression that they were cut by the seller to standardize the size of the hair fiber (Figure 3G–I).

In this work, the middle section was presented as a proper hair template to assess the damage in fibers because it showed the highest apparent homogeneity between tresses, presenting an accurate sample standardization for further characterization and an appropriate template for our work.

Following the optimization of the bleaching protocol, it was possible to observe the hair scale in the middle section, which was the bridge to identifying hair repair when treated with two benchmark products for this type of treatment. The differences were noticeable after the application of these products. Furthermore, the middle sections were considered to discern the repair effects induced by treatment with K18® and Olaplex®. Taking into consideration the successful optimization of the bleaching procedure that provoked visible damage to the hair surface, the impact of two commercial products, i.e., K18® and Olaplex® were further evaluated for morphology, color, structure, thermal, and mechanical properties as compared with the bleached samples used as a control.

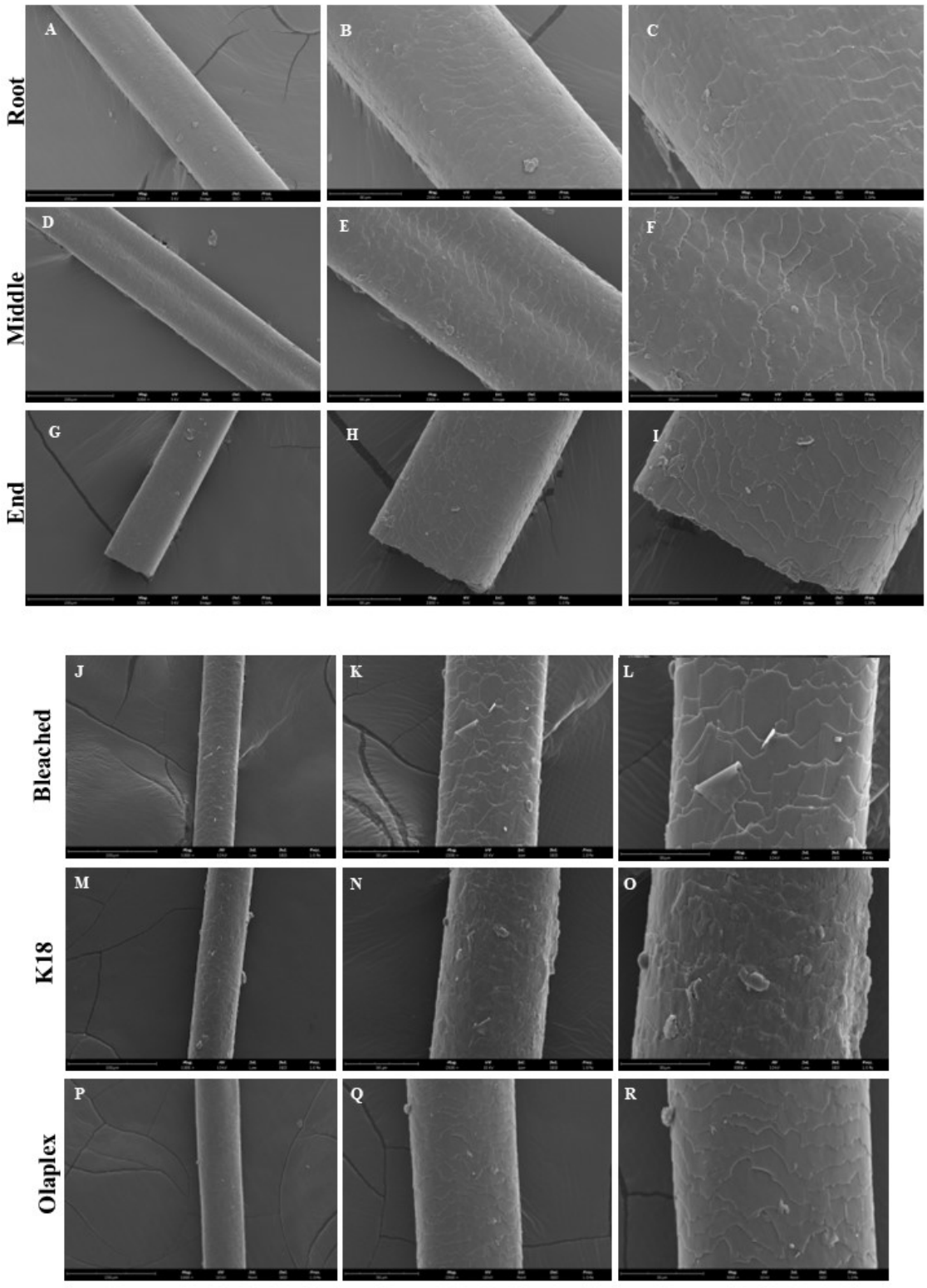

Figure 3. SEM micrographs of three distinct hair monofilament regions: (**A**–**C**) root, (**D**–**F**) middle, and end (**G**–**I**) of the bleached hair samples before bleaching optimization. SEM imaging to observe hair samples: (**J**–**L**) Bleached (**M**–**O**) K18®, and (**P**–**R**) Olaplex® of the surface morphology at 1000×, 2500×, and 5000× magnifications.

From Figure 3, it was seen that there was visible flaking on the fiber surface of bleached hair (Figure 3J–L), indicating considerable physical damage in the cuticle of the hair fiber. In the case of K18®, the observation suggested that this formulation formed a coating

on the surface of the fiber related to the presence of highly lipophilic ingredients in this product, including dicaprylyl ether. The morphology of hair fibers with K18® showed a reduction in visible flaking, making the fiber smoother (Figure 3M–O). This attribute is relevant and greatly appreciated by consumers, influencing their repetitive buying decisions [64]. For Olaplex® (Figure 3P–R), the presence of some visible flaking on the fiber surface was observed, likely due to the reduced amount used in the single application test, visible on the surface of this fiber. The Olaplex® product has a high water-based composition, making its ingredients likely to permeate easily across the cuticle. This suggests its potential to act within the core of the hair fibers. Despite both K18® and Olaplex® products showing good dispersibility, there were some perceptive differences in spreadability and absorption during application, indicating that the composition of each product impacts their distribution and interaction with the hair fiber surface. The amount of product to be applied may vary depending on the type of hair [65], as well as on ingredient composition and, therefore, final product viscosity. In this study, as there was no recommended dosage or specific application guidelines provided, it was used at 10% w/w of each product per hair tress and a standard application procedure to mitigate variability. Coderch et al. reported that bleaching reduces the amount of free lipids and the outermost hydrophobic lipid monolayer, weakening the cuticle and creating a hydrophilic surface with higher friction [37]. In this study, the addition of K18® significantly countered the reduction in lipids caused by the bleaching process. The differences observed align with the reported removal of the epicuticle during bleaching. Moreover, both Olaplex® and K18® formulations contain lipid excipients, which might contribute to an overestimation of the lipid content in treated hair samples. Our results suggest that the composition of amino acids that make up the keratin of hair and the putative pH alteration of the hair surface can influence the spreadability and absorption of the products. It has been reported that different hair dyes have distinct pH values [60,66]. Previous studies have indicated that different dyes and pH are important for the affinity with hair fiber [25]. This could provide an explanation for the observed differences in the coating of bleached-treated hair, as observed by SEM, and the effect of pH. Moreover, the bleaching procedure seems to modify the structure of the fiber surface, leading to a varied charge affinity for the treated products. The integrated system of hair exhibits unique chemical and physical properties. It is a multi-part morphological structure that functions as a single entity [28].

4.2.2. AFM Analysis

The surface topography of Bleached, K18®, and Olaplex® hair samples was assessed using Atomic Force Microscopy (AFM) as a complementary technique to SEM for the microstructure analysis of hair morphology. AFM technique enables the visualization of the heterogeneity across the cuticle surface and quantitatively assesses the morphological differences in the hair samples containing both commercial products in relation to the bleached one (used as a control). As described in the literature, the outermost layer of the hair fiber is composed of cuticle layers, which act as protective outer films. The cuticle is made up of five to ten overlapping scales, or cells, each of which is roughly 0.5 to 1.0 mm thick, for a total thickness between 2.5 to 10 mm [39,42]. From Figure 3, it was observed by 2D and 3D images that the surface of bleached hair has a distinct height (0–1.2 µm) with visible flaking on the fiber surface. There was a visible tendency of cuticle edges in a consistent interval of 10 µm approximately (Figure 4A,B). On the other hand, hair fiber containing K18® showed a smooth topography exhibiting a characteristic isotropic coating aspect and uniform height exhibiting a maximum of 2.5 µm (Figure 4C,D). The hair samples treated with Olaplex® revealed a less regular surface topography (Figure 4E,F), which was also confirmed by SEM. The deposition of Olaplex® upon the fiber surface seems to fill the gap with the cuticle and the porosity provoked by the bleaching protocol, which is present and well visible in the bleached sample. The Olaplex® product appears to be partially adsorbed into the fiber without differences in the highest height (1.2 µm) but with significant differences in hair topography relative to Bleached sample. This could be

due to its non-homogeneous deposition through the fiber surface. Hair fibers containing both K18® and Olaplex® products exhibited differences in the topography profile of the fibers compared to the bleached sample, suggesting that the deposition of both products successfully occurred on the fiber surface. The difference in how the two commercial products interact with the fiber surface, together with the perception during its application, suggests that both products have different spreadability properties on the hair surface, likely due to the different compositions and levels of penetration into the full extension of the hair fiber. Furthermore, the results of average roughness (Ra) (Figure 4G); RMS Roughness (Rq) (Figure 4H,I) Peak to valley Roughness (Rt, (Figure 4I)) were evaluated to quantify the changes in morphology.

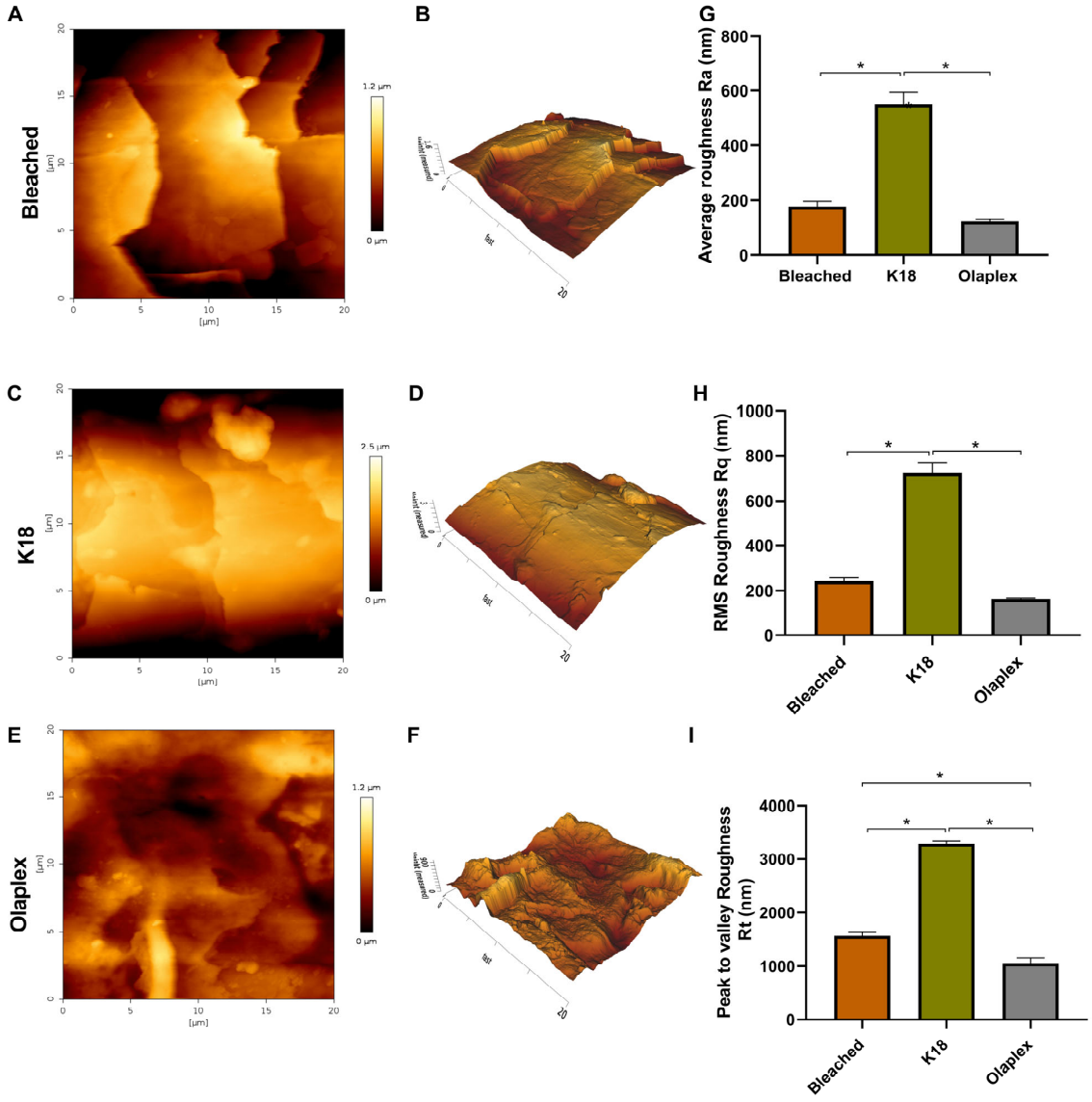

Figure 4. Atomic Force Microscopy (AFM) images and calculated surface roughness of Bleached, K18® and Olaplex®-treated hair samples. 2D and 3D topography images (20 µm × 20 µm) for the (**A**,**B**) Bleached hair sample; (**C**,**D**) K18® and (**E**,**F**) Olaplex®. Quantitative parameters of the topography for hair samples as (**G**) Average Roughness—Ra (nm); (**H**) RMS Roughness—Rq (nm); and (**I**) Peak to valley Roughness Rt (nm). The asterisks (*) denote a statistically significant difference ($p < 0.05$). Values represent the mean ± SD of at least two individual measurements.

From the results obtained in Figure 4, it was found statistically significant variations in average roughness between Bleached and K18® ($p < 0.05$), but also among K18® and

Olaplex® ($p < 0.05$) treatments, confirming the differences observed before on the deposition of both products upon the fiber surface.

4.2.3. Physical and Chemical Analysis

The relative density (g/cm^3) of Bleached hair showed the lowest values (1.31 ± 0.02) compared to the K18® (1.37 ± 0.06) and Olaplex® (1.39 ± 0.09) products, which are typical for human hair [67]. It is possible to see a slight increase in the density of hair fibers after application of the repair benchmark products; however, the differences observed were not significant among the tested hair samples (Figure 5A). This suggests that a potential modification in the porosity of hair after product application may occur without producing a relevant impact on the relative density of bleached hair.

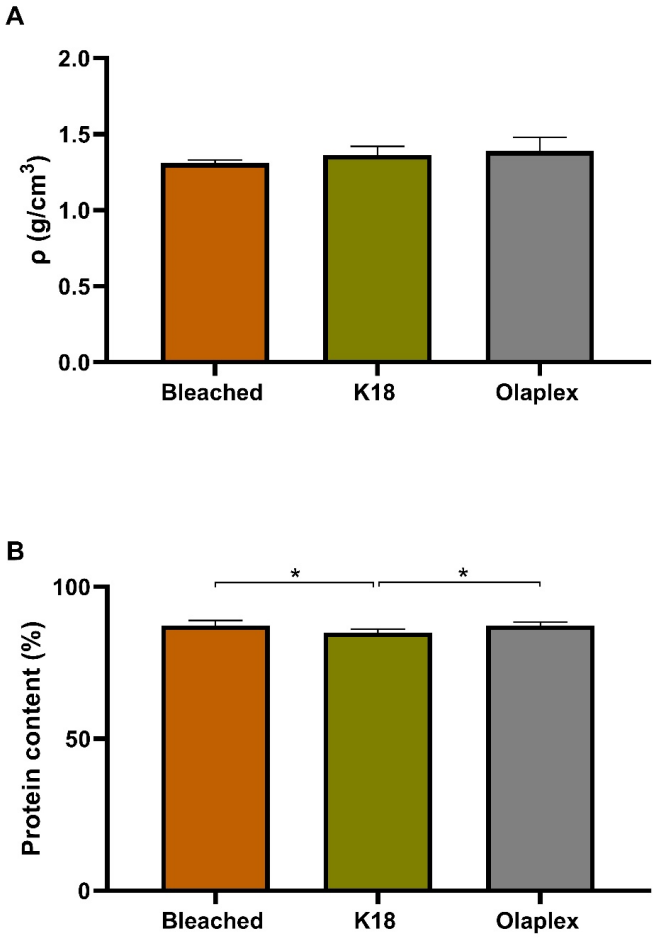

Figure 5. Density (**A**) and protein (**B**) content (%) results obtained for Bleached, K18®, and Olaplex® hair-treated samples. The asterisks (*) denote a statistically significant difference ($p < 0.05$). Values represent the mean ± SD.

Hair has a high protein content, mainly keratin, which has been described as playing a crucial role in its physical and chemical properties. Higher protein content (%) was verified in Bleached (87.32 ± 1.49) and Olaplex® (87.31 ± 1.04) compared to K18® (84.95 ± 1.07) treatments, revealing statistical differences ($p < 0.05$) (Figure 5B). The results suggested that water moisture was higher in the treated fibers, which were protected by the application of commercial products; consequently, the solid particles were present in a low amount. Thus, since the quantification of protein was performed in a wet state, the results showed a higher protein content in Bleached samples.

Functional Groups and Bonds

ATR-FTIR, Raman spectroscopy, and disulfide bonds were employed to examine keratin structural changes and hair chemical composition.

Based on the idea that all covalent bond transitions vibrate and absorb infrared light, Fourier-transform infrared spectroscopy analysis was performed [68]. ATR-FTIR reveals changes in the chemical bonds within the hair fiber, such as the presence of specific functional groups that indicate protein interactions or repair processes. For consumers, this translates into stronger and more resilient hair that is less prone to breakage and damage from styling or environmental factors. ATR-FTIR of hair samples was aimed at identifying the chemical differences observed between hair fiber containing K18® and Olaplex® in relation to Bleached samples. The spectra obtained for these samples are outlined in Figure 6A.

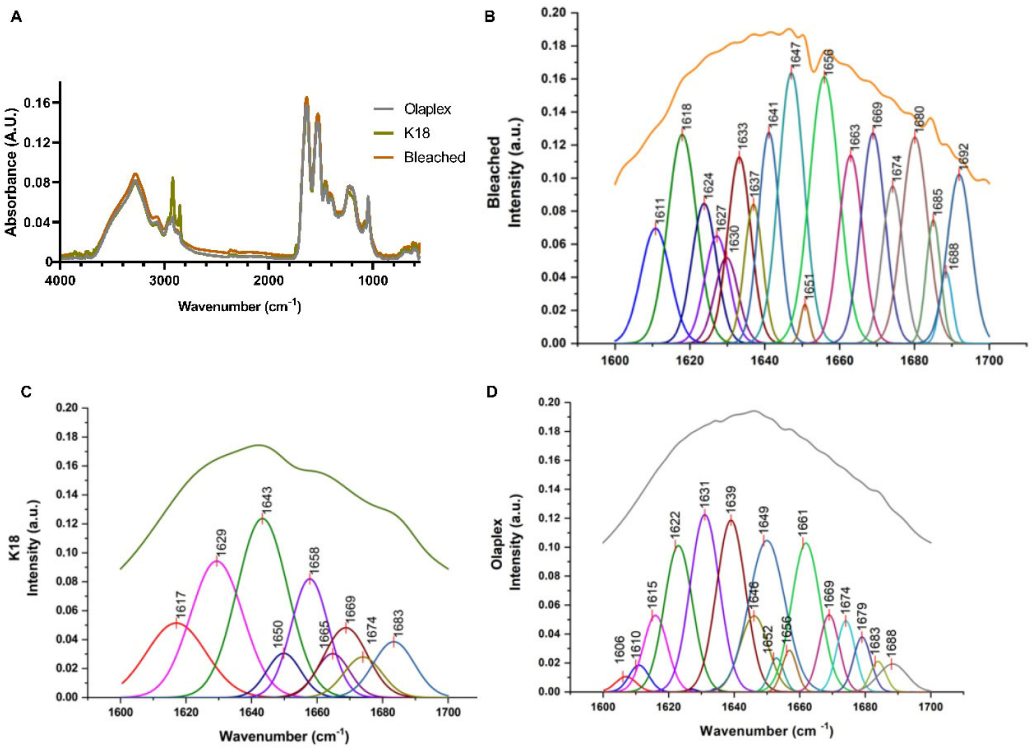

Figure 6. FTIR profiles of hair samples. (**A**) Overlapped FTIR spectra of Bleached, K18®, and Olaplex® hair samples. (**B**–**D**) Amide I deconvolution peaks of Bleached, K18®, and Olaplex®, respectively.

From Figure 6A, it was observed that there was a 99.2% overlapping between the ATR-FTIR spectrum of Olaplex® treated sample and the Bleached sample, whereas the K18® treated sample only presented a spectrum overlap of 84.6% with the bleached sample. Nonetheless, the main spectral differences seem to be associated with the peaks at 2960 cm^{-1}, 2920 $cm^{-1,}$ and 2850 $cm^{-1,}$ which are attributed to the stretching of C-H bonds. Therefore, the main differences observed are more likely due to the presence of some excipients in the K18® formulation than to any change in protein structure. In addition to the peptide and amino acids, the K18® formulation is composed of several excipients with C-H groups (e.g., surfactants, thickeners, and stabilizers). Previous studies have extensively reported that chemical degradation caused by bleaching initially leads to the oxidation of melanin, resulting in decoloration of the pigment and consequent hair clarification [69]. Afterward, proteinaceous hair content (with a prominent effect on highly oxidizable groupings, such as disulfide bonds, mainly present in cystine molecules) also becomes progressively oxidized [12]. Deconvolution of the amide I band was performed to assess hair protein integrity. Despite the high correlation between spectra, hidden peaks under the amide I band for K18®-and Olaplex®-treated samples and the bleached peak indicate different protein conformations for

each sample (Figure 6A). The most representative bands resulting from the deconvolution of amide I are shown in Figure 6B–D. From the analysis of the deconvoluted amide I peak, it was possible to observe that the a-helix band was similar for K18® (8.3%), Olaplex® (9.2%), and Bleached (9.6%) samples—Figure 6B–D. Nonetheless, Bleached sample presented the highest relative number of random coils (1647 cm^{-1}), indicating a high extent of protein denaturation and/or degradation. Indeed, the relative number of random coils decreased for both Olaplex® (3.6%) and K18® (2.8%) treated samples, suggesting a protein integrity recovery when compared with Bleached sample. Moreover, the Bleached sample presented a higher prevalence of antiparallel β-sheet/aggregated strands (1675–1695 cm^{-1} and 1610–1628 cm^{-1}) than K18® or Olaplex®, thus indicating some extent of protein reordination [70]. In fact, the relative area of the β-sheet in K18® and Olaplex® samples were 46.1% and 39.9%, respectively, in relation to 54.1% for Bleached sample [1,71]. The analysis of Ellman's test, on the other hand, revealed that K18® treatment led to the formation of new covalent bonds between the sulfur group of cysteines in keratin and other thiol groups, but this was not observed in Raman spectra (Figure 7A). Ellman's test indicated, however, that Olaplex® induced a significantly higher S-R bond establishment than K18® (Figure 7B). Both products have been reported to have different mechanisms of action. Indeed, the mechanism of action of Olaplex® consists of creating new, non-specific, S-R bonds, as bis-aminopropyl diglycol dimaleate, the active ingredient of Olaplex®, works as an acceptor molecule in a Michael addition reaction [62]. K18® is claimed to regenerate and form new S-S bonds. Thiol groups present in damaged hair are nucleophilic molecules, thus leading to the formation of S-R bonds. In summary, the fact that Olaplex® promotes the formation of unspecific bonds (S-R) is in accordance with the fact that the signal is higher in Ellman's test, but lower in the specific S-S Raman band. Statistical analysis confirmed differences in Bleached, K18®, and Olaplex® disulfide bond concentrations. However, bonds between Bleached and Olaplex® ($p < 0.0001$) were higher than between Bleached and K18® ($p < 0.0021$) or between K18® and Olaplex® ($p < 0.0015$). While K18® is reported by the commercializing brand to establish new disulfide bonds, Olaplex® showed a superior positive effect in the establishment of overall S-R bonds compared to the Bleached hair. These outcomes suggest that deeper bonds exist in Olaplex® than in the K18® product, also corroborated by SEM and AFM analysis, which indicates that penetration of Olaplex® across the fiber surface may be occurring.

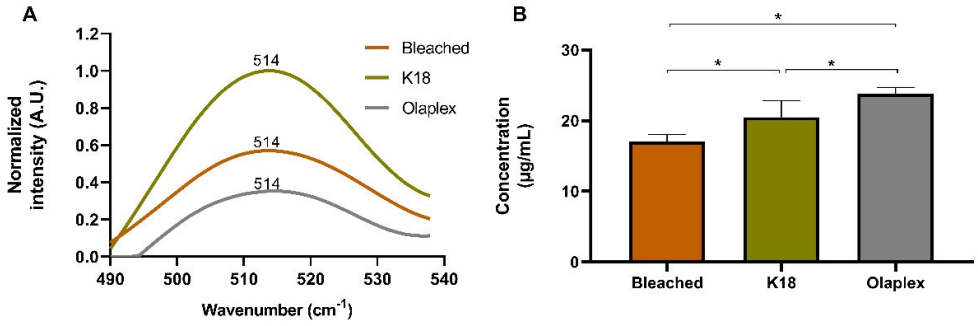

Figure 7. Disulfide bonds assessed by Raman spectroscopy (**A**) and S-R bonds were evaluated using Ellman's chemical procedure for the tested samples (**B**). Statistical significance between the samples was verified by an asterisk (*) symbol at $p < 0.05$.

4.2.4. Thermal Analysis

In Figure 8, the main thermal events of the hair samples are visible, whereas the Bleached, K18®, and Olaplex® samples revealed slight differences in the DSC thermogram.

Figure 8A–F demonstrate that the DSC profiles of the Bleached, K18®, and Olaplex® samples showed three characteristics of endothermic events. In Figure 8A, the main endothermic peaks of the hair samples are visible. The first peak (at around 130 °C) was assigned to the water evaporation peak, while peaks within the 230–245 °C range were

attributed to melting (or the number of ordered alpha-helices and decomposition of keratin or cystine decomposition) [72].

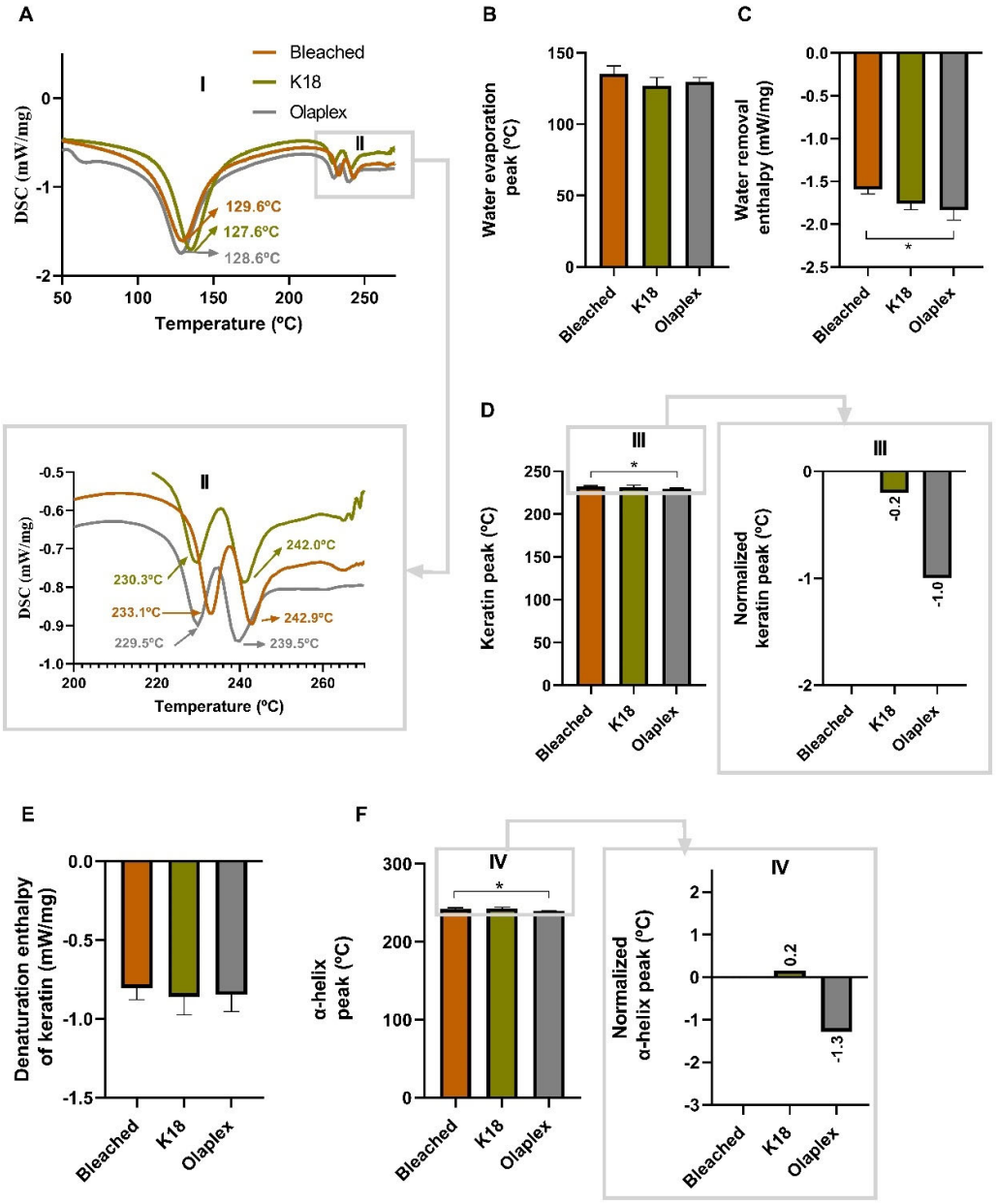

Figure 8. Thermal analysis of Bleached, K18®, and Olaplex® hair samples. (**A**) DSC thermograms of hair samples heated from 20 °C to 270 °C at a heating rate of 10 °C/min. The DSC curves for water evaporation and keratin denaturation (°C) are presented as I and II, respectively. (**B**–**F**) DSC results of water evaporation, water removal enthalpy (mW/mg), keratin peak and denaturation enthalpy of keratin (mW/mg), and α-helix of keratin peak for statistical analysis determination. III and IV symbols showed the variation of keratin peak in relation to Bleached. The asterisks (*) denote a statistically significant difference ($p < 0.05$). Values represent the mean ± SD ($n = 6$).

DSC analysis showed that the first peak had temperatures of 135.9 ± 5.6 °C, 127.00 ± 5.9 °C, and 129.9 ± 2.7 °C for Bleached, K18®, and Olaplex®, respectively; however, without statistically significant differences (Figure 8B). The corresponding enthalpy energy (mW/mg) values associated with the endothermic event of each sample were recorded, with values of −1.6 ± 0.05, −1.8 ± 0.07, and −1.8 ± 0.1 for Bleached, K18®, and Olaplex®, respectively (Figure 8C). The results suggested a tendency toward high enthalpy water

energy in the treated samples. However, only Olaplex®-treated samples demonstrated a significant difference from the bleached ones ($p < 0.05$). This was explained by the identical temperatures for water evaporation and by the similar energy needed to cause moisture evaporation. The results implied that the treated samples have a higher water content on the surface of the hair fiber due to the presence of these products compared to the Bleached ones. In addition, Olaplex® is rich in water ingredients compared to K18®. In cases of Bleached, the water content is likely present in the intra-fiber region.

DSC measures the thermal properties of hair, such as the denaturation temperature of keratin proteins, which indicates the structural integrity of hair. This translates for consumers into real advantages like stronger, smoother, and more damage-resistant hairs. This methodology helps to clarify the impact of products on everyday hair care.

From Figure 8A(II)), it is possible to observe a second endothermic event at 231.9 ± 1.5 °C, 231.5 ± 2.5 °C, and 229.6 ± 0.9 °C for Bleached, K18®, and Olaplex®, respectively, which accounted for the melting of keratin (Figure 8D). Keratin fibers are reported to be highly thermostable, with an intact structure that lasts until 200 °C [73]. Two distinct temperature ranges were identified by Cao [74]: one for water found in hair, which occurred until 200 °C, and another for the crystalline phase transition of α-keratin, occurring between 250 °C and 280 °C.

The Bleached samples showed the highest temperature for keratin denaturation compared to K18®-and Olaplex®-treated samples, which was in agreement with a previously reported study that demonstrated that the bleached hair exhibited an increase in the denaturation temperature of ca. 9 °C compared to that of virgin hair [75].

Statistical analysis showed that there were differences in the keratin peak between Bleached and Olaplex® samples, confirmed by one-degree differences in this peak (Figure 8D(III)). However, no significant differences ($p > 0.05$) were found for the enthalpy values among the Bleached (−0.8 ± 0.0 mW/mg), K18® (−0.9 ± 0.1 mW/mg), and Olaplex® (−0.8 ± 0.1 mW/mg) samples (Figure 8E). According to the literature [75], in virgin and bleached hair, the denaturation enthalpy was lower, with values of ca. 7.0 and 6.0 J mW/mg, respectively.

The last endothermic event observed for Bleached (242.33 ± 1.16 °C), K18® (242.60 ± 1.66 °C), and Olaplex® (239.17 ± 0.76 °C) were statistically different ($p > 0.05$) between Bleached and Olaplex® samples, demonstrating that Olaplex® treated hair denaturized at a lower temperature, suggesting minor thermal stability of α-helices (Figure 8F).

The TGA results showed hair weight loss (%) with increasing temperature and the corresponding derivative thermogravimetry (DTG %). DTG is frequently used to facilitate the reading of weight versus temperature. Figure 9 presents an example of a TGA replicate profile for each hair sample. Table 1 displays the main parameters obtained by TGA analysis expressed as mean and standard deviation ($n = 2$) for the Bleached, K18®, and Olaplex® samples.

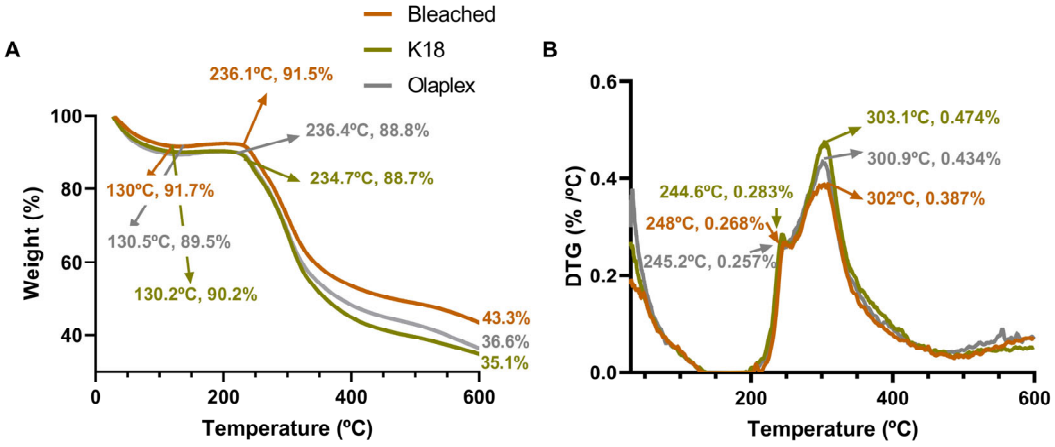

Figure 9. TGA analysis of K18® and Olapex® hair-treated samples in relation to the bleached sample (used as a control). (**A**) Weight (%) and (**B**) DTG (%, °C) curves of the TGA experiments.

Table 1. Thermogravimetric results expressed as the mean and standard deviation of two replicates for Bleached, K18®, and Olaplex®.

Samples	Event 1 (°C)	Event 2 (°C)	Max. Weight Loss (%)	Temp. 1 (°C)	DTG 1 (%)	Temp. 2 (°C)	DTG 2 (%)
Bleached	130.0 ± 0.0	235.6 ± 0.7	60.0 ± 4.7	246.0 ± 2.9	0.277 ± 0.013	301.9 ± 0.2	0.416 ± 0.041
K18	130.6 ± 0.0	235.2 ± 0.7	66.7 ± 2.5	244.4 ± 0.3	0.291 ± 0.011	303.5 ± 0.5	0.481 ± 0.009
Olaplex	130.5 ± 0.1	237.3 ± 1.3	67.0 ± 5.1	244.4 ± 1.1	0.267 ± 0.014	301.2 ± 0.4	0.453 ± 0.026

The hair samples showed identical TGA curves, presenting two main events, which are referred to in Table 1. The first event is related to moisture content, showing a loss of 9.0 ± 1.0%, 9.8 ± 0.0%, and 11.2 ± 1.0% for Bleached, K18®, and Olaplex®, respectively, at temperatures around 130 °C, which is associated with water loss (vaporization), as also observed in the DSC analysis (Figure 8). These differences can be explained by the intrinsic properties of the samples. In the case of Bleached sample, it has a lower water weight in its composition, likely due to the higher porosity of fiber and the consequent impact on the water loss. There were no statistically significant differences in the weight loss percentage ($p < 0.05$) for this event. In the literature, hydrolyzed proteins, which often contain free amino acids, are recognized for their humectant properties [36]. The information can be useful for understanding the K18® effect on hair fiber, as this formulation is made up of peptides that repair damage by reassembling broken polypeptide chains and disulfide bonds. Furthermore, the peptide's effect on hair, which typically increases the amount of loosely bonded water, is in contradiction to the trend of water content also reported by Popescu and Gummer [76]. The study by Qu et al. revealed that hair treated with hyaluronic acid had less loosely bound water compared to the Bleached samples when analyzed by TGA [17]. The application of K18® and Olaplex® products, which appeared to form a coating on the fiber surface, as observed by SEM, may play a role in moisture retention. On the other hand, Bleached hair, displaying an increased porosity caused by the absence of a coating layer, may facilitate water loss. For this reason, the Bleached hair sample may allow for faster water evaporation at lower temperatures compared to the treated samples. Gama et al. mentioned that the use of oxidants causes a decrease in external water content [36].

The second event was obtained at a temperature range of 235–240 °C, namely 235.6 ± 0.7, 235.2 ± 0.7, and 237.3 ± 1.3 °C for Bleached, K18®, and Olaplex®, respectively. The significant differences in keratin degradation were not statistically different ($p < 0.05$). The highest weight loss (%) occurred in Bleached samples (40.0 ± 4), followed by K18® (33.3 ± 2.5) and Olaplex® (33.0 ± 5.1). Bleached hair revealed a trend of lower structural stability caused by a minor number of bonds. However, these differences were not statistically significant compared to the treated samples. We recommend that continuous application of the tested products could demonstrate a prominent effect.

The two DTG temperatures obtained were very similar to the weight loss (%) in Table 1). DTG is the derivative curve of TG, where DTG distinguished two degradation peaks between 244 and 246 °C and 301–304 °C for the hair samples. According to Monteiro et al., the second and third mass loss stages are related to the denaturation of hair keratin and the organic degradation of hair microfibrils and matrix at 290.7 °C and 307.6 °C [77]. The latter temperature range, namely, the derivative of thermal analysis (DTG2), showed the temperature where the maximum rate of mass loss occurred, with values of 0.416 ± 0.041, 0.481 ± 0.009, and 0.453 ± 0.026 for Bleached, K18®, and Olaplex®, respectively. No statistical differences were found between the results. In addition, the temperature of 350–550 °C is related to the complete degradation of the hair keratin carbonic chains [36].

4.2.5. Mechanical Behavior

The thickness or diameter of the hair fiber seems to exert an influence on the mechanical parameters [3]. Considering that the thickness of each monofilament was accurately measured

by microscopy analysis prior to the mechanical evaluation. Bleached samples usually display high porosity and lower strength. The hair monofilament analysis is a challenging technique due to the variability in the samples. However, after optimization of the protocol, it was possible to present robust results in Figure 10A–C. It was observed that strength declined as hair diameter increased [67]. The results revealed that the thickness of our specimens had a diameter typically between 45 and 110 µm for Bleached, K18®, and Olaplex® samples, with certain variability in each single hair fiber. When we analyzed the mean and standard deviation parameters of these hair samples (Figure 10D), we observed small differences in the average thickness of Bleached (68.7 ± 18.1), K18® (69.7 ± 17.8), and Olaplex® (75.8 ± 18.9) hair fibers. Yang and collaborators reported a fiber average thickness between 27–81 µm in individuals with straight, curly, and wavy hair appearances [78]. Compared to Caucasian hair, Asian hair has a higher tensile force due to its larger diameter [79]. Additionally, thinner hair in Caucasians is associated with a lighter and more yellow-colored appearance [80]. Apparently, the thickness seems to be higher in the treated samples, in the Olaplex® ones, compared to the Bleached samples. However, these differences were not statistically significant ($p < 0.05$). The results found here are in line with previously published results showing hair fibers with a diameter of 50–100 µm [3,81].

From Figure 10, it is possible to clearly observe an increase in the tensile strength for hair-treated samples compared to Bleached ones. Remarkably, the monofilament fibers with superior thickness exhibited a higher tensile strength. Commonly, healthy hair has a visibly higher tensile strength, while damaged hair tends to break more easily with regular brushing [17]. It is well established in the literature that hair mechanical properties can change depending on several factors, including humidity, temperature, pollution, and chemical compounds [3,82]. In addition, McMichael et al. stated that weathering from different hair care techniques and genetic susceptibility can cause hair fragility that results in breakage [83]. Water content and hydrogen bonding play major roles in the mechanical properties of hair [35,84,85]. In this study, the potential of Olaplex® and K18® commercial products to rebuild internal bonds compromised by the bleaching process was explored, thereby enhancing the mechanical properties of hair, in particular, the fiber's mechanical strength and extensibility. Olaplex® showed superior thickness and the highest tensile strength and extensibility (Figure 10C–F), suggesting that the product may play a role in the core of the fiber, thus affecting the intrinsic mechanical properties. In the case of K18®, the pattern was similar (Figure 10B,D–F); however, the effect was less prominent compared to Olaplex®. SEM and AFM observations showed that K18® acts at a superficial level without a significant effect on the core of the hair fiber. From Figure 10E, it is possible to observe that Olaplex® and K18® led to an increase of 47.6% and 19.5%, respectively, in the tensile strength in relation to Bleached samples (Figure 10E). These results may be related to the increased establishment of the S-S and S-R bonds reported above. This effect was pronounced and statistically significant ($p < 0.05$) for hair fibers treated with Olaplex®. Previous studies have reported that the cortex of the hair is mainly responsible for its mechanical strength, which is weakened by bleaching [86], thus suggesting that Olaplex® may be acting at the cortex level. In fact, Olaplex® led to a strong increase in the strength of hair fibers, likely due to the bonds created between the free tiol groups and bis-aminopropyl diglycol dimaleate, as an active compound. In other studies, it was reported that low-molecular-weight hyaluronate (average MW~42 kDa) compounds enhanced the mechanical characteristics of overbleached hair [17], as observed here for Olaplex®. Malinauskyte et al. [25] showed that the mechanical properties of hair were improved by the ability of medium- and high-molecular-weight keratin peptides to rebuild internal chemical bonds and replenish moisture. Furthermore, the best ability to interact with a keratin peptide model was demonstrated using PepE, PepG, and KP peptides based on human hair keratin fragments and KAPs. These peptides significantly improve the suppleness and tensile strength of badly damaged hair [82]. Interestingly, hair fibers' elasticity and mechanical resistance to elongation, blending, and twisting are both attributed to the strongly cross-linked amino acid cystine [12,37,87].

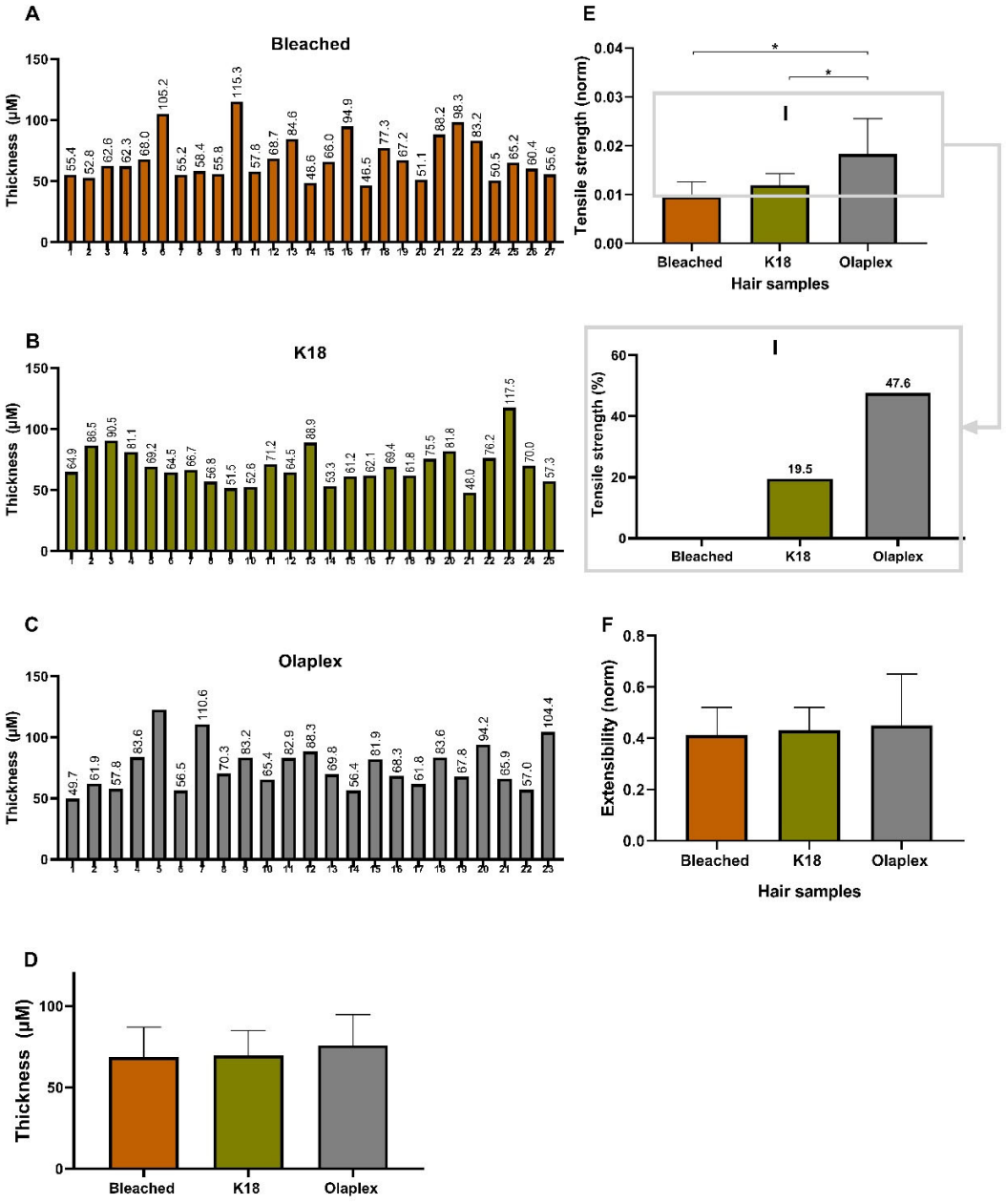

Figure 10. Physical and mechanical properties of hair fibers. (**A**–**C**) Thickness (µm) of Bleached, K18®, and Olaplex®, respectively. (**D**) Mean and Standard deviation of hair samples (n = 25). (**E**) Tensile strength (N), I symbol shows the variation of tensile strength in relation to Bleached, and (**F**) Extensibility (mm) of the hair strands obtained by Tensile tests. The asterisks (*) denote a statistically significant difference ($p < 0.05$).

In the case of hair fiber extensibility, a soft tendency of Olaplex® to extend is observed, but this observation was not confirmed statistically by the data analyzed (Figure 10F).

5. Conclusions

The specific bleaching time and temperature conditions were determined, considering the products used and the specific salon practices. Moreover, we investigated the bibliographic literature and found that the bleaching process is not a standard method.

In this study, a bleached protocol was successfully developed and implemented to provoke sufficient damage in hair as a standard procedure for evaluating the potential repair effect of commercial benchmark products on the appearance and morphological, structural,

and mechanical properties of hair fibers. For this purpose, several complementary analytical tools have been used to deliver detailed information on how commercial repair products are acting. Firstly, an external and faster characterization of the fiber surface in terms of color, brightness, and lightness was provided, which was later correlated with a morphological and topography analysis using SEM and AFM techniques. From the primary analysis performed, it was possible to verify that the formulated bleaching protocol is a suitable framework for evaluating the properties of hair and the distinct characteristics influenced by each product within the hair fiber, as well as for selecting the middle section of the fiber as the most appropriate and reproducible section to visualize hair damage. Then, the hair fiber was characterized in detail in terms of its density, protein content and integrity, intrinsic bonds, moisture content, thermal stability, and mechanical properties to comprehend the nuanced differences between the samples treated with K18® and Olaplex® and the bleached sample. Olaplex® is a commercial product that mostly increases hair brightness and lightness, which are crucial attributes that greatly affect consumers' choices. Using AFM and SEM techniques, it was possible to perceive significant variations in the fiber surface and topography among the bleached samples used as the control and treated samples using both commercial benchmarks in a single application of each product. Olaplex® formed a visible inner sheet, filling the empty spaces with evidence of deeper penetration across the fiber surface. This led to an improvement in the disulfide linkage network, although more relevant to the formation of new bonds, increasing the strength of the hair fiber and consequently its mechanical properties, confirming the role of this product in the core of the fiber. In turn, K18® had a more superficial effect with the formation of an external layer above the fiber, which played a role in the improvement of fiber smoothness and recovery of more extrinsic bonds. Both tested products have a short-term effect on hair fibers and being suitable alternatives to diminish hair the damage to hair after the bleaching. This study deepened the understanding of a product's contribution to fiber properties and established a stronger correlation between various complementary approaches to characterizing hair fibers (Figure 11). The analytical tools confirmed the efficacy and action of the two benchmark products on damaged hair. The outlined set of tools for evaluating product properties may represent a step forward toward the strategic development of claims made by beauty industry products, potentially shaping the future certification of marketing claims by beauty brands.

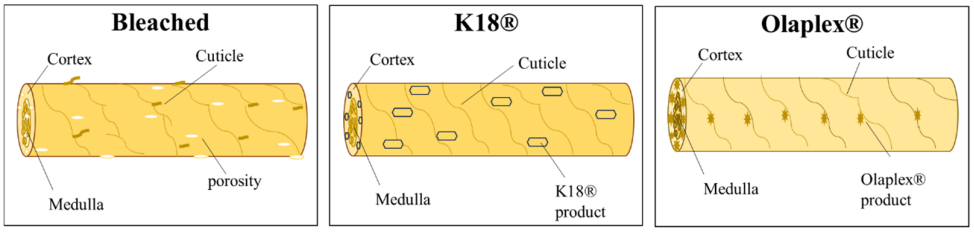

Figure 11. Schematic representation of Bleached, K18® and Olaplex® after full characterization of hair fiber.

Author Contributions: Conceptualization, E.M. and Ó.L.R.; methodology, E.M., P.C., A.B.R., C.F.P., F.C., R.V., J.M. and Ó.L.R.; writing—original draft preparation, E.M.; writing—review and editing, E.M., P.C., A.B.R. and Ó.L.R. All authors have read and agreed to the published version of the manuscript.

Funding: Project co-financed by the European Regional Development Fund (ERDF) through the Operational Program for Competitiveness and Internationalization (POCI) supported by Amyris Bio Products Portugal, Unipessoal Ltd. and Escola Superior de Biotecnologia—Universidade Católica Portuguesa through the Alchemy project "Capturing High Value from Industrial Fermentation Bio Products" (POCI-01-0247-FEDER-027578). We would also like to thank the scientific collaboration under the FCT project UIDB/50016/2020.

Institutional Review Board Statement: Not applicable.

Informed Consent Statement: Not applicable.

Data Availability Statement: The data obtained during this study are available at the corresponding author's request.

Conflicts of Interest: The authors declare that they have no known competing financial interests or personal relationships that could have appeared to influence the work reported in this paper.

References

1. Di Foggia, M.; Boga, C.; Micheletti, G.; Nocentini, B.; Taddei, P. Structural investigation on damaged hair keratin treated with α, β-unsaturated Michael acceptors used as repairing agents. *Int. J. Biol. Macromol.* **2021**, *167*, 620–632. [CrossRef] [PubMed]
2. Goyal, N.; Jerold, F. Biocosmetics: Technological advances and future outlook. *Environ. Sci. Pollut. Res.* **2023**, *30*, 25148–25169. [CrossRef] [PubMed]
3. Benzarti, M.; Tkaya, M.B.; Mattei, C.P.; Zahouani, H. Hair mechanical properties depending on age and origin. *World Acad. Sci. Eng. Technol.* **2011**, *74*, 471–477.
4. Fink, B.; Neuser, F.; Deloux, G.; Röder, S.; Matts, P.J. Visual attention to and perception of undamaged and damaged versions of natural and colored female hair. *J. Cosmet. Dermatol.* **2013**, *12*, 78–84. [CrossRef] [PubMed]
5. Hong, S.R.; Lee, S.M.; Lim, N.R.; Chung, H.W.; Ahn, H.S. Association between hair mineral and age, BMI and nutrient intakes among Korean female adults. *Nutr. Res. Pract.* **2009**, *3*, 212–219. [CrossRef] [PubMed]
6. Almohanna, H.M.; Ahmed, A.A.; Tsatalis, J.P.; Tosti, A. The Role of Vitamins and Minerals in Hair Loss: A Review. *Dermatol. Ther.* **2019**, *9*, 51–70. [CrossRef]
7. Flanagan, R.F.; Cai, J.X. Untangling the Link between Gastroparesis, Micronutrient Deficiency, and Hair Loss. *Dig. Dis. Sci.* **2023**, *68*, 1086–1088. [CrossRef]
8. LaTorre, C.; Bhushan, B. Nanotribological effects of hair care products and environment on human hair using atomic force microscopy. *J. Vac. Sci. Technol. A Vac. Surf. Film.* **2005**, *23*, 1034–1045. [CrossRef]
9. McMullen, R.; Schiess, T.; Kulcsar, L.; Foltis, L.; Gillece, T. Evaluation of the surface properties of hair with acoustic emission analysis. *Int. J. Cosmet. Sci.* **2021**, *43*, 88–101. [CrossRef]
10. McMullen, R.L.; Kelty, S.P. Investigation of human hair fibers using lateral force microscopy. *Scanning* **2001**, *23*, 337–345. [CrossRef]
11. Igarashi, K.; Maeda, K. Research on hair bleach that causes less hair damage and smells less pungent than ammonium hydroxide. *Cosmetics* **2018**, *5*, 39. [CrossRef]
12. Robbins, C.R.; Robbins, C.R. *Chemical and Physical Behavior of Human Hair*; Springer: Berlin/Heidelberg, Germany, 2012; Volume 4.
13. Kojima, T.; Yamada, H.; Isobe, M.; Yamamoto, T.; Takeuchi, M.; Aoki, D.; Matsushita, Y.; Fukushima, K. Compositional changes of human hair melanin resulting from bleach treatment investigated by nanoscale secondary ion mass spectrometry. *Ski. Res. Technol.* **2014**, *20*, 416–421. [CrossRef] [PubMed]
14. Pötsch, L. A discourse on human hair fibers and reflections on the conservation of drug molecules. *Int. J. Leg. Med.* **1996**, *108*, 285–293. [CrossRef] [PubMed]
15. Imai, T. The influence of hair bleach on the ultrastructure of human hair with special reference to hair damage. *Okajimas Folia Anat. Jpn.* **2011**, *88*, 1–9. [CrossRef] [PubMed]
16. Kim, K.-H.; Kabir, E.; Jahan, S.A. The use of personal hair dye and its implications for human health. *Environ. Int.* **2016**, *89*, 222–227. [CrossRef]
17. Qu, W.; Guo, X.; Xu, G.; Zou, S.; Wu, Y.; Hu, C.; Chang, K.; Wang, J. Improving the mechanical properties of damaged hair using low-molecular weight hyaluronate. *Molecules* **2022**, *27*, 7701. [CrossRef]
18. Robbins, C.R.; Robbins, C.R. Bleaching and oxidation of human hair. In *Chemical and Physical Behavior of Human Hair*; Springer: Berlin/Heidelberg, Germany, 2012; pp. 263–328.
19. Tinoco, A.; Martins, M.; Cavaco-Paulo, A.; Ribeiro, A. Biotechnology of functional proteins and peptides for hair cosmetic formulations. *Trends Biotechnol.* **2022**, *40*, 591–605. [CrossRef]
20. Guthrie, J.; Kazlauciunas, A.; Rongong, L.; Rush, S. The characterisation of treated and dyed hair. *Dye. Pigment.* **1995**, *29*, 23–44. [CrossRef]
21. Camargo, F.B., Jr.; Minami, M.M.; Rossan, M.R.; Magalhaes, W.V.; Porto Ferreira, V.T.; Maia Campos, P.M.B.G. Prevention of chemically induced hair damage by means of treatment based on proteins and polysaccharides. *J. Cosmet. Dermatol.* **2022**, *21*, 827–835. [CrossRef]
22. Pereira-Silva, M.; Martins, A.M.; Sousa-Oliveira, I.; Ribeiro, H.M.; Veiga, F.; Marto, J.; Paiva-Santos, A.C. Nanomaterials in hair care and treatment. *Acta Biomater.* **2022**, *142*, 14–35. [CrossRef]
23. Tinoco, A.C.M. The Potential of Multifunctional Proteins and Peptides for Hair Protection and Coloring. Ph.D. Thesis, Universidade do Minho, Braga, Portugal, 2020.
24. Neelima, T.; Riyamol, K.; Harikumar, N. Science and Technology of Hair Fibers. In *Handbook of Biomass*; Springer: Berlin/Heidelberg, Germany, 2023; pp. 1–19.
25. Malinauskyte, E.; Shrestha, R.; Cornwell, P.; Gourion-Arsiquaud, S.; Hindley, M. Penetration of different molecular weight hydrolysed keratins into hair fibres and their effects on the physical properties of textured hair. *Int. J. Cosmet. Sci.* **2021**, *43*, 26–37. [CrossRef] [PubMed]

26. Morita, T.; Kitagawa, M.; Yamamoto, S.; Sogabe, A.; Imura, T.; Fukuoka, T.; Kitamoto, D. Glycolipid biosurfactants, mannosylerythritol lipids, repair the damaged hair. *J. Oleo Sci.* **2010**, *59*, 267–272. [CrossRef] [PubMed]
27. Fan, C.; Shi, J.; Wei, X.; Xie, Z.; Cheng, M.; Cao, X.; Zhou, Y.; Zhan, Y.; Yan, Y. Bioinspired peptides designed for hair perming and dyeing with potential for repair. *Acta Biomater.* **2023**, *168*, 440–457. [CrossRef] [PubMed]
28. Dias, M.F.R.G. Hair cosmetics: An overview. *Int. J. Trichology* **2015**, *7*, 2–15. [CrossRef]
29. Grosvenor, A.; Deb-Choudhury, S.; Middlewood, P.; Thomas, A.; Lee, E.; Vernon, J.; Woods, J.; Taylor, C.; Bell, F.; Clerens, S. The physical and chemical disruption of human hair after bleaching—Studies by transmission electron microscopy and redox proteomics. *Int. J. Cosmet. Sci.* **2018**, *40*, 536–548. [CrossRef]
30. Dias, M.F.R.G.; de Almeida, A.M.; Cecato, P.M.R.; Adriano, A.R.; Pichler, J. The shampoo pH can affect the hair: Myth or reality? *Int. J. Trichology* **2014**, *6*, 95–99. [CrossRef]
31. Barve, K.; Dighe, A. *The Chemistry and Applications of Sustainable Natural Hair Products*; Springer: Berlin/Heidelberg, Germany, 2016.
32. Marsh, J.; Brown, M.; Felts, T.; Hutton, H.; Vatter, M.; Whitaker, S.; Wireko, F.; Styczynski, P.; Li, C.; Henry, I. Gel network shampoo formulation and hair health benefits. *Int. J. Cosmet. Sci.* **2017**, *39*, 543–549. [CrossRef]
33. Hashim, P.; Mat Hashim, D. A review of cosmetic and personal care products: Halal perspective and detection of ingredient. *Pertanika J. Sci. Technol.* **2013**, *21*, 281–292.
34. Gray, J. Hair care and hair care products. *Clin. Dermatol.* **2001**, *19*, 227–236. [CrossRef]
35. Benzarti, M.; Pailler-Mattei, C.; Jamart, J.; Zahouani, H. The effect of hydration on the mechanical behaviour of hair. *Exp. Mech.* **2014**, *54*, 1411–1419. [CrossRef]
36. Da Gama, R.M.; Balogh, T.S.; França, S.; Dias, T.C.S.; Bedin, V.; Baby, A.R.; do Rosário Matos, J.; Velasco, M.V.R. Thermal analysis of hair treated with oxidative hair dye under influence of conditioners agents. *J. Therm. Anal. Calorim.* **2011**, *106*, 399–405. [CrossRef]
37. Coderch, L.; Alonso, C.; García, M.T.; Pérez, L.; Martí, M. Hair Lipid Structure: Effect of Surfactants. *Cosmetics* **2023**, *10*, 107. [CrossRef]
38. Wang, N.; Barfoot, R.; Butler, M.; Durkan, C. Effect of surface treatments on the nanomechanical properties of human hair. *ACS Biomater. Sci. Eng.* **2018**, *4*, 3063–3071. [CrossRef] [PubMed]
39. Bhushan, B. Nanoscale characterization of human hair and hair conditioners. *Prog. Mater. Sci.* **2008**, *53*, 585–710. [CrossRef]
40. Sinclair, R.D. Healthy hair: What is it? *J. Investig. Dermatol. Symp. Proc.* **2007**, *12*, 2–5. [CrossRef]
41. Rogers, G.E. Known and unknown features of hair cuticle structure: A brief review. *Cosmetics* **2019**, *6*, 32. [CrossRef]
42. Fellows, A.P.; Casford, M.T.; Davies, P.B. Nanoscale molecular characterization of hair cuticle cells using integrated atomic force microscopy—Infrared laser spectroscopy. *Appl. Spectrosc.* **2020**, *74*, 1540–1550. [CrossRef]
43. Wolfram, L.J. Human hair: A unique physicochemical composite. *J. Am. Acad. Dermatol.* **2003**, *48*, S106–S114. [CrossRef]
44. Humphry, R.; Wang, N.; Durkan, C. Site-specific variations in surface structure and Young's modulus of human hair surfaces at the nanometer scale as induced through bleach treatment. *J. Mech. Behav. Biomed. Mater.* **2022**, *126*, 105001. [CrossRef]
45. Garcia, M.L.E.J.A.; Yare, R.S. Normal cuticle-wear patterns in human hair. *J. Soc. Cosmet. Chem.* **1978**, *29*, 155.
46. Bhattarai, D.; Banday, A.Z.; Sadanand, R.; Arora, K.; Kaur, G.; Sharma, S.; Rawat, A. Hair microscopy: An easy adjunct to diagnosis of systemic diseases in children. *Appl. Microsc.* **2021**, *51*, 18. [CrossRef] [PubMed]
47. Fernandes, C.; Medronho, B.; Alves, L.; Rasteiro, M.G. On Hair Care Physicochemistry: From Structure and Degradation to Novel Biobased Conditioning Agents. *Polymers* **2023**, *15*, 608. [CrossRef]
48. Malepfane, N.; Muchaonyerwa, P. Hair from different ethnic groups vary in elemental composition and nitrogen and phosphorus mineralisation in soil. *Environ. Monit. Assess.* **2017**, *189*, 76. [CrossRef] [PubMed]
49. Yu, Y.; Yang, W.; Wang, B.; Meyers, M.A. Structure and mechanical behavior of human hair. *Mater. Sci. Eng. C* **2017**, *73*, 152–163. [CrossRef] [PubMed]
50. Samanta, A.; Bhattacharya, M.; Dalui, S.; Acharya, M.; Das, P.S.; Chanda, D.K.; Acharya, S.D.; Sivaraman, S.K.; Nath, S.; Mandal, A.K.; et al. Nanomechanical responses of human hair. *J. Mech. Behav. Biomed. Mater.* **2016**, *56*, 229–248. [CrossRef]
51. De Cássia Comis Wagner, R.; Kiyohara, P.K.; Silveira, M.; Joekes, I. Electron microscopic observations of human hair medulla. *J. Microsc.* **2007**, *226*, 54–63. [CrossRef]
52. Deedrick, D.W.; Koch, S.L. Microscopy of hair part 1: A practical guide and manual for human hairs. *Forensic Sci. Commun.* **2004**, *6*, 1.
53. Ly, B.C.K.; Dyer, E.B.; Feig, J.L.; Chien, A.L.; Del Bino, S. Research techniques made simple: Cutaneous colorimetry: A reliable technique for objective skin color measurement. *J. Investig. Dermatol.* **2020**, *140*, 3–12.e11. [CrossRef]
54. Ordóñez-Santos, L.E.; Martínez-Girón, J.; Arias-Jaramillo, M.E. Effect of ultrasound treatment on visual color, vitamin C, total phenols, and carotenoids content in Cape gooseberry juice. *Food Chem.* **2017**, *233*, 96–100. [CrossRef]
55. *ASTM D792−20*; Standard Test Methods for Density and Specific Gravity (Relative Density) of Plastics by Displacement. ASTM International Organization for Standardization: West Conshohocken, PA, USA, 2020.
56. Cruz, C.F.; Azoia, N.G.; Matamá, T.; Cavaco-Paulo, A. Peptide–Protein interactions within human hair keratins. *Int. J. Biol. Macromol.* **2017**, *101*, 805–814. [CrossRef]
57. *ISO-5079-2020.(E)*; Textile Fibres—Determination of Breaking Force and Elongation at Break of Individual Fibres. 3rd ed. International Organization for Standardization: Geneva, Switzerland, 2020.

58. Payne, C.E.; Rockson, A.; Ashrafi, A.; McDonald, J.A.; Bethea, T.N.; Barrett, E.S.; Llanos, A.A. Beauty Beware: Associations between Perceptions of Harm and Safer Hair-Product-Purchasing Behaviors in a Cross-Sectional Study of Adults Affiliated with a University in the Northeast. *Int. J. Environ. Res. Public Health* **2023**, *20*, 7129. [CrossRef] [PubMed]
59. Lee, J.; Kwon, K.H. Considering the risk of a coloring shampoo with the function of gray hair cover cosmetology and skin barrier: A systematic review. *Health Sci. Rep.* **2023**, *6*, e1271. [CrossRef]
60. Yun, K.; Ahn, C. Effect of surfactant type on the dyeability and color resistance of semi-permanent basic hair dye. *Fash. Text.* **2023**, *10*, 4. [CrossRef]
61. Xu, L.; Dong, J. Click chemistry: Evolving on the fringe. *Chin. J. Chem.* **2020**, *38*, 414–419. [CrossRef]
62. Pressly, E.D.; Hawker, C.J. Methods for Fixing Hair and Skin. 2015. Available online: https://patentimages.storage.googleapis.com/e6/92/5f/e237aaac6b0003/US9095518.pdf (accessed on 24 July 2024).
63. Vaughn, M.; Van Oorschot, R.; Baindur-Hudson, S. Hair color measurement and variation. *Am. J. Phys. Anthropol. Off. Publ. Am. Assoc. Phys. Anthropol.* **2008**, *137*, 91–96. [CrossRef] [PubMed]
64. Murugan, D.B. A Study on Rural Customers' Perception—A Case of Shampoo. *SSRN Electron. J.* **2010**. [CrossRef]
65. Labarre, L.; Squillace, O.; Liu, Y.; Fryer, P.J.; Kaur, P.; Whitaker, S.; Marsh, J.M.; Zhang, Z.J. Hair surface interactions against different chemical functional groups as a function of environment and hair condition. *Int. J. Cosmet. Sci.* **2023**, *45*, 224–235. [CrossRef]
66. Morel, O.; Christie, R.M.; Greaves, A.; Morgan, K.M. Enhanced model for the diffusivity of a dye molecule into human hair fibre based on molecular modelling techniques. *Color. Technol.* **2008**, *124*, 301–309. [CrossRef]
67. Yang, W.; Yu, Y.; Ritchie, R.O.; Meyers, M.A. On the strength of hair across species. *Matter* **2020**, *2*, 136–149. [CrossRef]
68. Barba, C.; Oliver, M.A.; Martí, M.; Kreuzer, M.; Coderch, L. Lipid distribution on ethnic hairs by Fourier transform infrared synchrotron spectroscopy. *Ski. Res. Technol.* **2022**, *28*, 75–83. [CrossRef]
69. Smith, R.; Garrett, B.; Naqvi, K.; Fülöp, A.; Godfrey, S.; Marsh, J.; Chechik, V. Mechanistic insights into the bleaching of melanin by alkaline hydrogen peroxide. *Free Radic. Biol. Med.* **2017**, *108*, 110–117. [CrossRef] [PubMed]
70. Jackson, M.; Mantsch, H.H. The use and misuse of FTIR spectroscopy in the determination of protein structure. *Crit. Rev. Biochem. Mol. Biol.* **1995**, *30*, 95–120. [CrossRef]
71. Essendoubi, M.; Andre, N.; Granger, B.; Clave, C.; Manfait, M.; Thuillier, I.; Piot, O.; Ginestar, J. New approach for hair keratin characterization: Use of the confocal Raman spectroscopy to assess the effect of thermal stress on human hair fibre. *Int. J. Cosmet. Sci.* **2022**, *44*, 588–601. [CrossRef] [PubMed]
72. Oliver, M.A.; Coderch, L.; Carrer, V.; Barba, C.; Marti, M. Ethnic hair: Thermoanalytical and spectroscopic differences. *Ski. Res. Technol.* **2020**, *26*, 617–626. [CrossRef] [PubMed]
73. Istrate, D.; Popescu, C.; Möller, M. Non-Isothermal Kinetics of Hard α-Keratin Thermal Denaturation. *Macromol. Biosci.* **2009**, *9*, 805–812. [CrossRef] [PubMed]
74. Cao, J. Melting study of the α-form crystallites in human hair keratin by DSC. *Thermochim. Acta* **1999**, *335*, 5–9. [CrossRef]
75. Lima, C.R.R.d.C.; Machado, L.D.B.; Velasco, M.V.R.; Matos, J.d.R. DSC measurements applied to hair studies. *J. Therm. Anal. Calorim.* **2018**, *132*, 1429–1437. [CrossRef]
76. Popescu, C.; Gummer, C. DSC of human hair: A tool for claim support or incorrect data analysis? *Int. J. Cosmet. Sci.* **2016**, *38*, 433–439. [CrossRef]
77. Monteiro, V.F.; Maciel, A.; Longo, E. Thermal analysis of caucasian human hair. *J. Therm. Anal. Calorim.* **2005**, *79*, 289–293. [CrossRef]
78. Yang, F.-C.; Zhang, Y.; Rheinstädter, M.C. The structure of people's hair. *PeerJ* **2014**, *2*, e619. [CrossRef]
79. Franbourg, A.; Hallegot, P.; Baltenneck, F.; Toutaina, C.; Leroy, F. Current research on ethnic hair. *J. Am. Acad. Dermatol.* **2003**, *48*, S115–S119. [CrossRef]
80. Vaughn, M.R.; Brooks, E.; van Oorschot, R.A.; Baindur-Hudson, S. A comparison of macroscopic and microscopic hair color measurements and a quantification of the relationship between hair color and thickness. *Microsc. Microanal.* **2009**, *15*, 189–193. [CrossRef] [PubMed]
81. Sayahi, E.; Harizi, T.; Msahli, S.; Sakli, F. Physical and mechanical properties of T unisian women hair. *Int. J. Cosmet. Sci.* **2016**, *38*, 470–475. [CrossRef] [PubMed]
82. Cruz, C.F.; Martins, M.; Egipto, J.; Osório, H.; Ribeiro, A.; Cavaco-Paulo, A. Changing the shape of hair with keratin peptides. *RSC Adv.* **2017**, *7*, 51581–51592. [CrossRef]
83. McMichael, A.J. Hair breakage in normal and weathered hair: Focus on the Black patient. *J. Investig. Dermatol. Symp. Proc.* **2007**, *12*, 6–9. [CrossRef]
84. Wei, G.; Bhushan, B. Nanotribological and nanomechanical characterization of human hair using a nanoscratch technique. *Ultramicroscopy* **2006**, *106*, 742–754. [CrossRef]
85. Barba, C.; Méndez, S.; Martí, M.; Parra, J.; Coderch, L. Water content of hair and nails. *Thermochim. Acta* **2009**, *494*, 136–140. [CrossRef]

86. Dawber, R. Hair follicle structure, keratinisation and the physical properties of hair. In *Diseases of the Hair and Scalp*, 3rd ed.; Dawber, R., Ed.; Blackwell Science: Oxford, UK, 1997; pp. 23–50.
87. Tanaka, S.; Iimura, H.; Sugiyama, T. Study of the test method of reduction and recovery of disulfide bond in human hair. *J. Soc. Cosmet. Chem. Jpn.* **1992**, *25*, 232–239. [CrossRef]